An Introduction to Cloud Microphysics (1)

by
P Ryder

METEOROLOGICAL OFFICE
4 JUL 1990
LIBRARY

1. The properties of water substance

1.1 Some Elementary Ideas on the Molecular Structure of Water

Water is the most common and most widely distributed liquid on the surface of the Earth, but it was wrongly considered for a long time as a standard of liquids. It presents, on the contrary, aberrant physical characteristics which make it a most singular substance.

The state and the properties of a substance depend on its composition. Liquid water, ice, and water vapor are made up of the same molecules (H_2O), and differ only in the interactions exercised by these molecules. These interactions, weak in the gaseous state, become important in the liquid state, and even more so in the solid state.

The water molecule with the chemical formula H_2O is made up of two hydrogen atoms tied to one oxygen atom. The molecular bond results from the sharing of the two solitary hydrogen atom electrons by the oxygen atom to complete the outer shells of both elements.

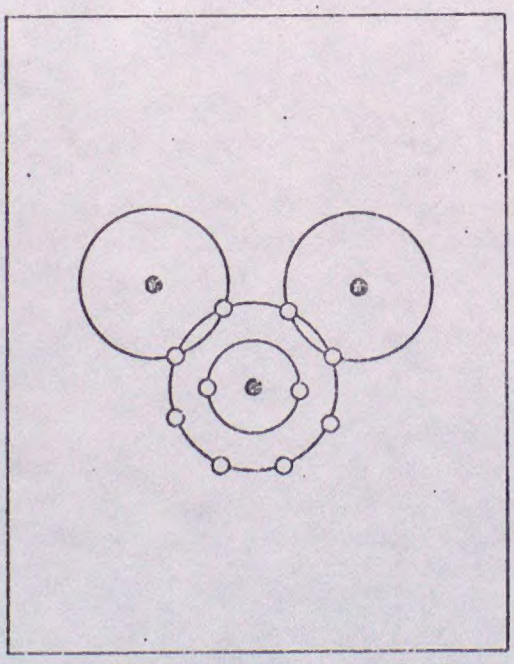

Two hydrogen atoms combined with one oxygen atom forming a molecule of water (H_2O).

The angle $\widehat{HOH}$ of the isosceles triangle, of which the nucleus of the three atoms occupy the corners, is 105°. The water molecule, like, for example, the hydrogen molecule H–H, is naturally electronically neutral; nevertheless, the covalent linking furnished by the shared electrons

differs from the H–H link by creating a polar character. In effect, the oxygen has more affinity for the electrons than the hydrogen. The electronic density is greater in the vicinity of the nucleus of the oxygen than in that of the hydrogen. Thus the center of gravity of the positive and negative charges does not coincide. As a result the water molecule is polar; it is the equivalent of a small electrical dipole and possesses a permanent electrical moment. When several water molecules are present, the positively charged hydrogens attract the electronic cloud surrounding an oxygen molecule; the molecules having then a tendency to unite. The fact that in each molecule the angle $\widehat{HOH}$ has a value of about 105°, that is close to the angle at the center of a regular tetrahedron (109°28'), favours a tretrahedric arrangement of molecules in the solid state (ice).

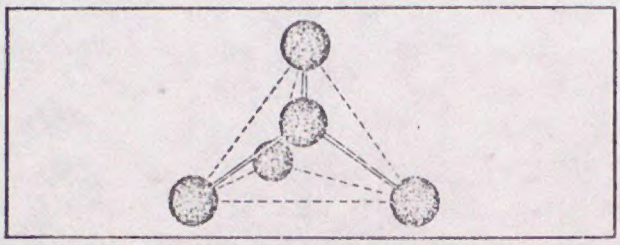

Tetrahedral arrangement of oxygen atoms.

One oxygen, at the center of the tetrahedron, is bound to four oxygens placed at each of the corners by the intermediary of a hydrogen atom. Two of these liaisons are those of covalence; the two others, called "hydrogen bonds", are of an electrostatic nature. These latter are loose, of weaker energy than those of the covalent bonds but sufficient to assure the stability of the crystalline edifice and to be responsible for certain properties of the water.

The result of each oxygen being the center of a small tetrahedron, is that the tetrahedrons assemble themselves into a regular crystalline structure of hexagonal symmetry (see below). This assembly, rather loose and hollow, offers lacunae in which other molecules, smaller and of a different nature, are able to insert themselves to form what chemists call "insertion compounds" or "clathrate".

Furthermore, these "hydrogen bonds" oppose free movement of the molecules. It is necessary to break them up, consequently expending a certain energy, to pass from the solid state to the liquid state, where a certain number of these bonds still remain, then to the gaseous state where the molecules are free and very mobile. The supplementary energy necessary for the rupture of the hydrogen bonds is supplied by the addition of heat. This explains why the fusion temperature of water and its boiling point can be much higher than those of analogous compounds (H_2S–H_2Se) of which the molecules are not linked between themselves by "hydrogen bonds".

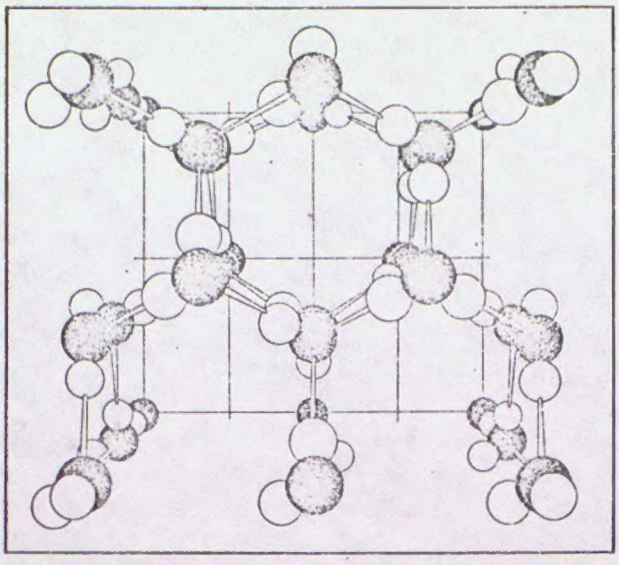

Crystalline structure of hexagonal symmetry; arrangement of tetrahedral groups of molecules.

In the melting of ice, the rupture of a certain number of "hydrogen bonds" provokes the collapse of the crystalline edifice with compression of the molecules. From this, the volume decreases and the density increases until a temperature (4°C) is reached beyond which thermal expansion compensates for the effect of this compression. It is for these reasons that we observe a density maximum in pure water at 4°, under normal pressure, and that ice is less dense than water.

1.2 Physical Characteristics of Water

Among the exceptional properties which spring from the particular constitution of water, those which play a role in the chain of geophysical phenomena may be summarized thus:

(1) Water is the sole natural compound which exists in the three states in the condition of temperature and pressure which are found on Earth; the liquid state being the most common.

(2) Water has a high specific heat, linked, on the one hand, to the fact that one of its constituents, hydrogen, has the highest specific heat of all the elements, and on the other hand, to the presence of "hydrogen bonds". It has, moreover, an important heat of fusion (83 cal), of vaporization (537 cal), a thermal conductivity, high for a liquid (but, in spite of that, fairly low and close to that of brick) and low viscosity. From this it presents a strong thermal inertia, is opposed to rapid variations of temperature, and is an excellent agent for the transport and storage of caloric energy.

(3) Water, because of its high dielectric constant, is the natural milieu where the greatest number of substances, whether they be mineral or organic, in a gaseous, liquid, or solid state, are able to dissolve and interact.

(4) The freezing water is accompanied by an increase in volume of about 10% and because of this:

(a) ice floats on water;

(b) freezing splits the partitions of cells in animal or plant and porous rock;

(c) ice, a crystalline lacunar system, is plastic, and glaciers and inlandis slip towards the sea.

(5) Like all liquids, water is only slightly compressible, but if this compressibility can be neglected in the first approximation, it nevertheless exists, and is responsible for the fact that sea level is in the neighbourhood of 30 m lower than it would be if the compressibility were nil. Aside from this, the coefficient of compressibility presents an anomoly; it diminishes with rising temperature and reaches a minimum at around 50°C.

(6) The surface tension of water (73 dynes/cm at 20°C at normal pressure) is the highest of all liquids. This characteristic influences the formation of drops of water as well as waves.

(7) The surface of water in a liquid state reflects only a small part of luminous radiation and absorbs much solar heat. In the solid state, on the other hand, it reflects 50% and even 70 to 80% if it is in the form of crystals of fresh snow.

To the physical considerations set forth above it is still appropriate to add the fact that the atoms composing the water molecule are, from a chemical point of view, singularly active.

The dielectric constant of a liquid measures its capacity to neutralize the attraction between electric charges. Water has a very high dielectric constant (80), which signifies that two opposing electric charges attract each other in water with a force 80 times smaller than in the air. This high dielectric constant, due to the polarity of the molecule and to the union of molecules between them, causes the water to possess a remarkable dissolving power for ionic substances. A positive ion draws the negative electronic clouds which surround the oxygen atoms of nearby water molecules. A negative ion, on the contrary, attracts the positive side of the water molecule. Positive ion and negative ion are thus separated and isolated by the oriented water molecules surrounding them. These water molecules, grouped around the ion, and of which the number determines the dimensions of this ion, form a sort of cage neutralising and stabilizing the ions.

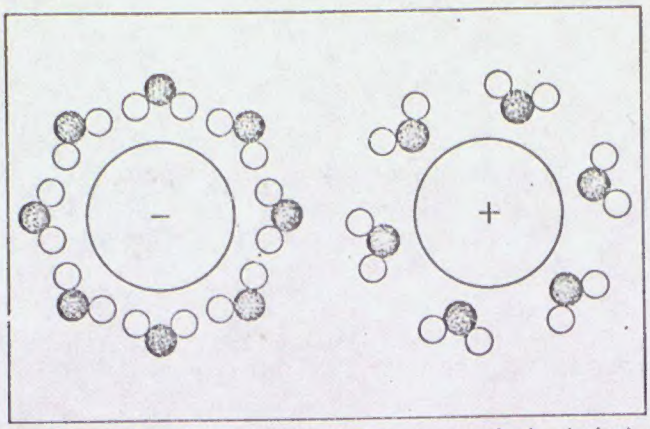

Orientation of water molecules in the presence (*left*) of a negative ion (anion), or (*right*) a positive ion (cation).

It was pointed out above that water appears to be a quasi-universal solvent. Now certain physical properties of a solvent are modified by the presence of dissolved matter. These properties, called colligatives, are principally osmotic pressure, vapor tension, and boiling and freezing tempertures.

Thermodynamically linked, these properties depend not only on the number of molecule-grams of dissolved matter (Raoult's law) but also on the state of dissociation of the molecules of the dissolved substances and the ionic interaction in the case of electrolytes.

This has several important consequences. Thus the presence of dissolved salts lowers the freezing point of sea water (salinity $\sim$ 35‰) to $-$ 1.9°C. However for a cloud physisicist the effect of a solute in lowering the equilibrium saturation vapour pressure is of major significance. It provides an important link between dry particulate aerosol and the aerosol we know as cloud and precipitation.

2. Properties of atmospheric aerosol

2.1 Dimensions

The dimension of a small molecule or an atom is of the order of 10^{-8} cm. There is no generally accepted definition of how large clusters of molecules must become to be particles, but those with an inferred radius of about 10^{-7} cm have been detected. Particles of this size undergo large Brownian movements which allow them to reach the walls of any reasonably sized container in a few seconds or at best a few minutes. Particles of this size also coagulate very quickly with larger particles for the same reason. One could envisage the distinction between molecules and particles being based on adhesions to clean walls, as molecules do not so adhere in general. Our knowledge of adhesive forces is not sufficient to make this a very practical definition however.

10^{-6} cm represents a more stable and permanent size at which reasonable storage times are possible and coagulation at atmospheric concentrations is not excessively fast. The limit of direct observation of particles by electron microscopy occurs in this region.

10^{-5} cm is considered to be 'large' in the context of atmospheric aerosol. It is a regime little affected by Brownian movement and by gravitational settling. Particles of this size are likely to have the longest survival as individuals since, as we shall see, both diffusive and inertial coagulative processes are inefficient. 10^{-5} cm also represents a size of particle which is very difficult to produce directly. It is virtually impossible to grind material to this degree of fineness while condensation from the vapour phase (except with very volatile materials) tends to produce smaller particles.

10^{-4} cm (1 μm) In the parlance of atmospheric aerosol this is the small end of the 'giant' particles in the atmosphere. Haze particles are of this sort of size. The fall speed under gravity of a 1 μm particles is only about 1 mm every 5 seconds but even this slight sedimentation amounts to 20 m per day - and fall speed increases quadratically in this size region. These particles can readily be observed on a surface under moderate magnification but those slightly smaller have unusual optical properties because of their similarity to the wavelength of visible light.

10^{-3} cm (10 μm). This is the characteristic dimension of cloud droplets. The fall speed of a 10 μm particle of density 2 gm cm^{-3} - under normal surface conditions, is about 2 cm sec^{-1}, so in a couple of minutes most 10 μm particles in an average room would fall out under gravity. Particles of this size lying on a suitable surface can be seen with the naked eye.

10^{-2} cm (100 μm). This is the size of fine drizzle drops with a fall speed of about 1 ms^{-1}. Drops of this size are produced by sea spray, and such dry particles are raised by dust storms - neither travel far from their source.

10^{-1} cm (1 mm). A typical raindrop. Note that $\sim 10^{6}$ cloud droplets are necessary to form one such raindrop. Inevitably the volume concentration is small, $< 10\ m^{-3}$, even in moderate rain.

1 cm; falling raindrops break up through hydrodynamic effects around 0.5 cm. However solid hydrometers such as hail, graupel and snow can attain this size.

10 cm. Occasionally hail particles of this size are reported. They inevitably cause severe damage.

2.2 Size distributions of aerosol $\lesssim$ 100 μm

Experimental observations suggest that, at least over a part of the atmospheric particle size range, power laws tend to be found, especially when distributions are averaged. Repeated reference is made in the literature to the 'Junge distribution'. His work in the 1940's and early 50's showed that in populated continental areas observed particle distributions from a few tenths of a micron to a few tens of microns, tended to give a constant particulate volume per log radius interval. Thus he found approximately equal particulate volumes between say 0.4 and 0.6 μm, between 0.6 and 0.9 μm, between 1 and 1.5 μm and between 4 and 6 μm. The volume of 4 to 6 μm particles is one thousand times the volume of 0.4 to 0.6 μm particles; this implies a thousand times fewer of the large particles. This tendency of the natural aerosol (sampled mainly at the earth's surface) can be expressed as

$$r^3 \, (dN/d \log r) = \text{constant}$$

where N is the total concentration of aerosol particles of radius less than r. The number of particles per unit radius interval in this size range is proportional to r^{-4}.

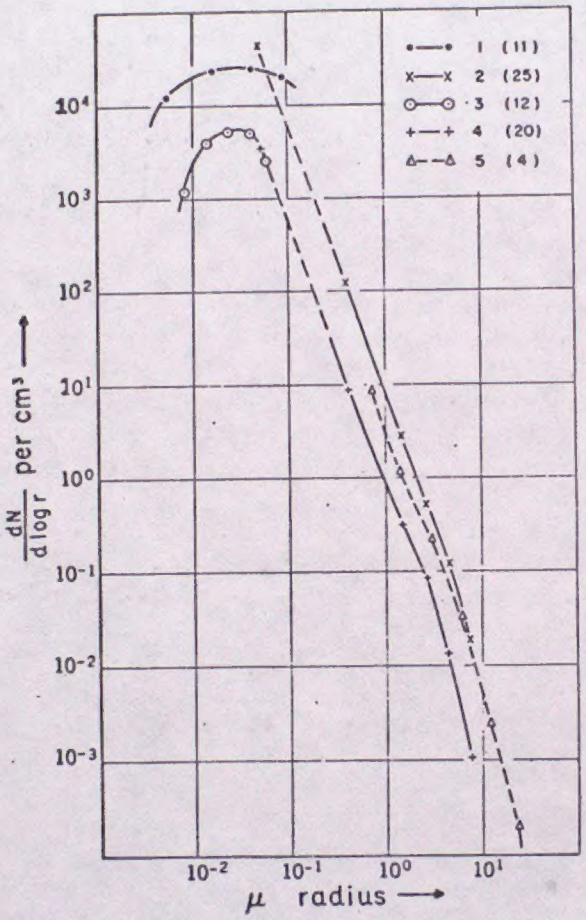

Complete size distributions of natural aerosols, average data (Junge, 1953, 1955 a). Frankfurt/Main, curves 1, 2, and 5. Curve 1, ion counts converted to nuclei numbers. Curve 2, data from impactors. The point below 0.1 μ radius was obtained from the total Aitken nuclei number under the assumption that the radius interval of the Aitken nuclei is $\Delta \log r = 1.0$. Curve 5, average sedimentation data over a period of 11 days. Curves 1, 2, and 5 are *not* simultaneous. Curves 3 and 4 are simultaneous measurements at the Zugspitze, 3000 meters above s.l., and correspond to curves 1 and 2 for Frankfurt. The figures in parentheses give the number of individual measurements. The dashed curves between 8×10^{-2} and 4×10^{-1} μ are interpolated.

Over the oceans conditions are fundamentally different. Woodcock (1953) has found that there is a clearly defined and apparantly universal relationship between number and size of maritime aerosol greater than

about 1 μm radius. He found that the aerosol consist of sea spray particles. The total concentration, peak of the mass distribution and the upper limit of the size of the aerosol are all found to increase with wind strength.

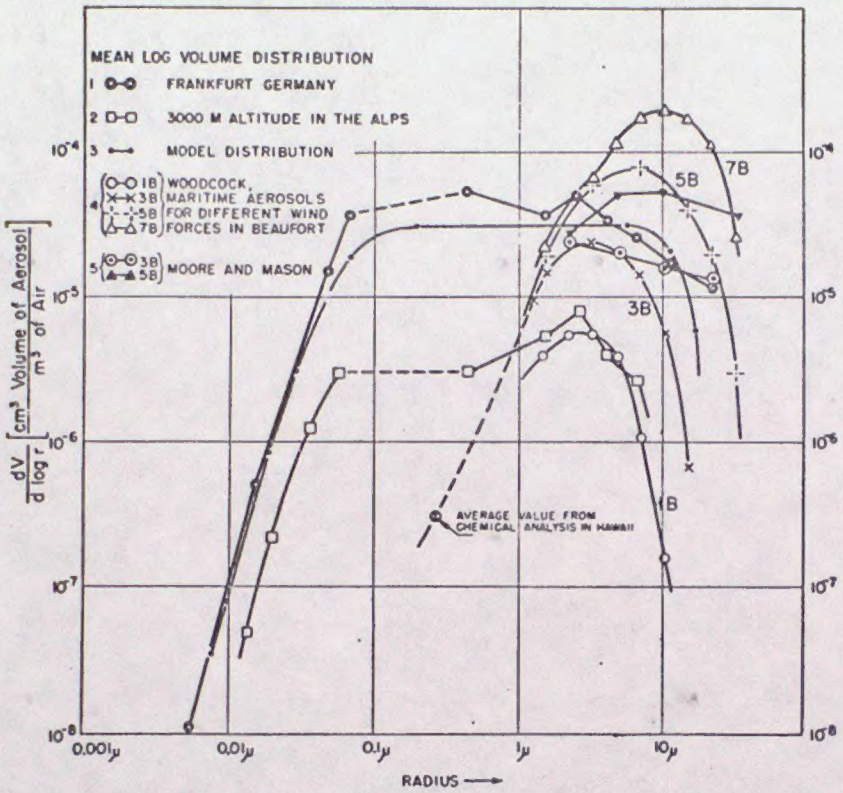

Log radius-volume distribution for continental and maritime aerosols, (Woodcock, 1953; Moore and Mason, 1954; Junge, 1956). Curve 3B is extrapolated to a point determined by chemical analysis. The curve of Frankfurt is approximated by a " model " distribution.

Instruments which measure particles of all sizes - say from 10^{-7} to 10^{-3} cm in radius - would indicate particle concentrations which are most commonly in thousands and tens of thousands per cm^3.

Concentrations in the hundreds per cm^3 are found in clean, remote sites and aloft. Alternatively counts exceeding 10^5 and even 10^6 cm^{-3} are found in urban air samples. The attached diagram shows data obtained on a flight of the MRF Hercules aircraft by an instrument which measures the total number of particles in the size range $\sim 5.10^{-7}$ to 10^{-5}cm. These were obtained at 3,000 ft in a South Westerly airflow over the North Irish Sea and Inner Hebrides. The contrast between the effects of urban-industrial activity of Northern Ireland and the much cleaner air with a North Atlantic fetch is very obvious.

Despite these large concentrations it is important to realise that they represent rather small contributions to the chemical budget of the atmosphere. Thus some 0.01 μg m^{-3} might be tied up in particulates but the typical gaseous concentration of H_2O is 10^4 to 10^7 μg m^{-3}, that of CO_2 6 10^5 μg m^{-3}, SO_2 20 μg m^{-3} and NH_3 10 μg m^{-3}.

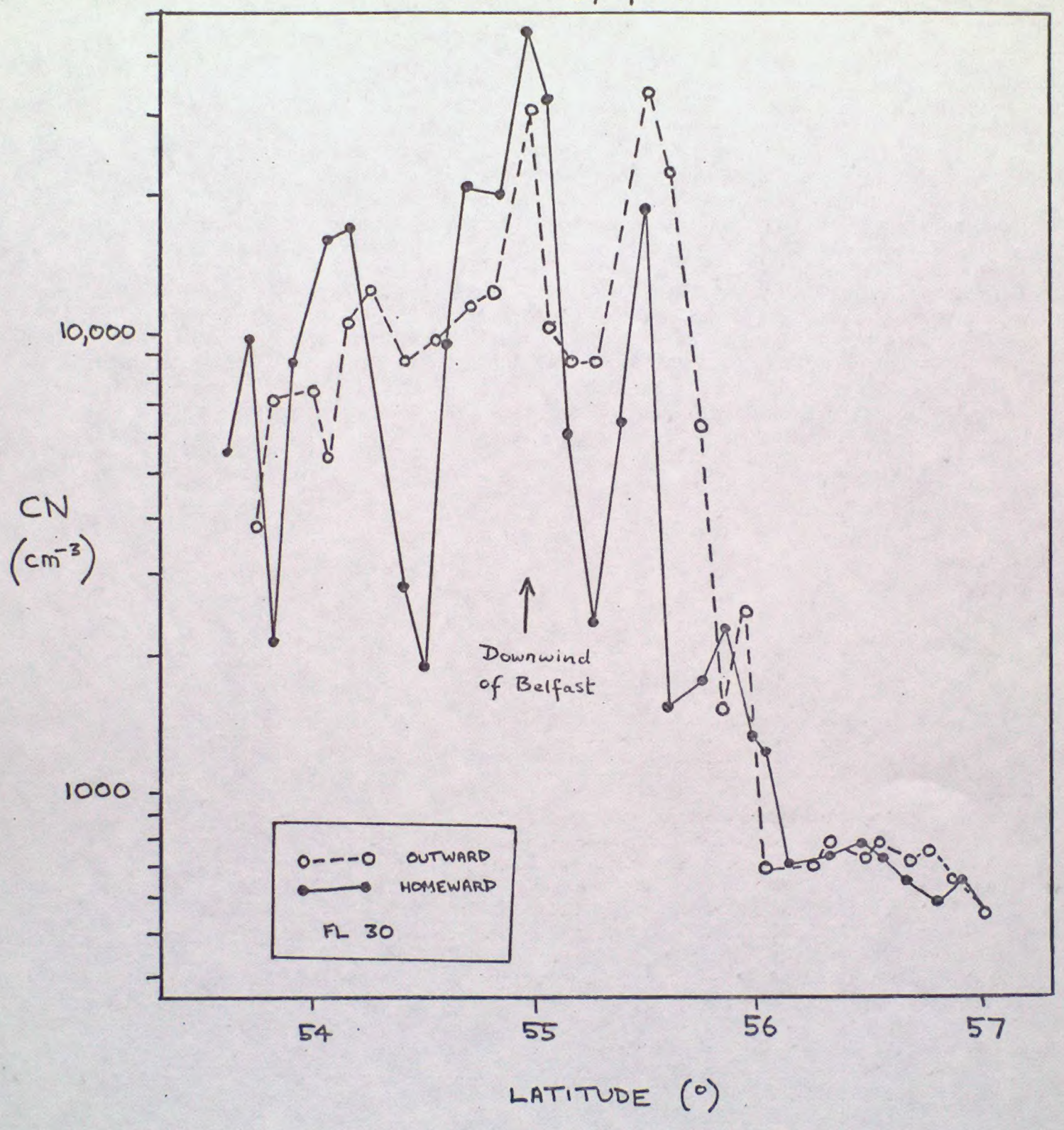
H337 10/7/79
10,000
1000
CN
(cm⁻³)
Downwind
of Belfast
OUTWARD
HOMEWARD
FL 30
54
55
56
57
LATITUDE (°)

Most, but not all, drop size distributions measured in many different types of clouds under a variety of meteorological conditions exhibit a characterisitic shape. Generally the concentration rises sharply from a low value to a maximum and then decreases more gently towards larger sizes. Such a characterisitic shape can be reasonably well approximated to by a lognormal or gamma distribution function. Other convenient empirical representations have been developed, eg. by Best (1951); none have other than descriptive value and represent average distributions in some sense. In a subsequent lecture Caughey and Brown respectively will discuss the drop size distribution in cumulus cloud and fog in some detail. The diagram below exhibits the main features of typical drop size distributions in well developed clouds of the types indicated. The presence of significant numbers of large drops ($r > 30\ \mu m$) only in vigorous convective cloud is worthy of note. Another common feature but not apparent from the diagram is the tendency for high drop concentrations in continental clouds to be associated with narrow drop size spectra and small drop sizes, while in maritime clouds low drop concentrations are associated with broad size spectra and large drop sizes. The characteristics of the larger atmospheric particluates, precipitation size drops, ice crystals, snowflakes, hail etc will be discussed in the second lecture.

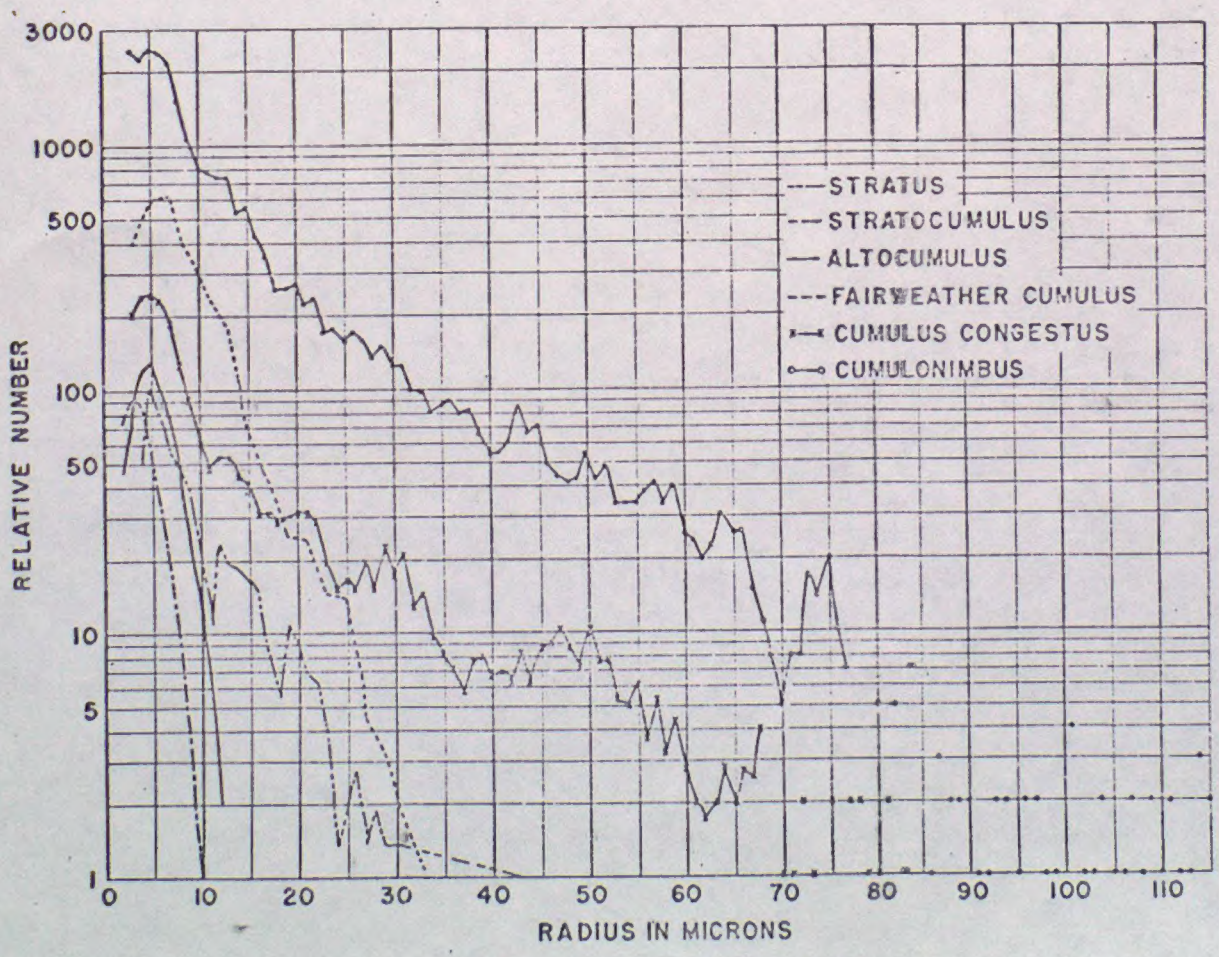

Average droplet spectra for different cloud types.

3 The physics of formation and early growth of aerosol

New particles can be formed from:

(a) disruption or splintering of existing solid material
(b) disruption of existing liquid surfaces
(c) by condensation (or sublimation) from the vapour.

Subsequent growth in the atmosphere is initially by addition of further vapour molecules, but eventually coagulative processes become important. Discussion of the latter is deferred to the second part of this introduction.

3.1 Disruption of solid material

The detachment of particles by the movement of air over a granular surface is not straightforward because in the absence of external mechanical agitation the wind speed decreases as the surface is approached. As a result there is little left in the way of a force to lift particles into the air. Bagnold (1941) carried out the definitive work in this subject. His experiments demonstrated that there is a critical value of the Reynold's Number $Re = \frac{du^*}{\nu}$ (d = particles diameter, u^* is the so called friction velocity and ν is the kinematic viscosity of air) below which the flow around a particle is smooth and therefore not conducive to its disturbance. Re_{CRIT} is ~ 3.5. This is a necessary condition, but the velocity required to lift the particle may be assessed crudely by equating the moment of the weight of the particle about its point of contact with the underlying grains, with the moment of the aerodynamic force. Thus

$$u^* \geq A \sqrt{\frac{\rho_p}{\rho_a} dg} \qquad \text{where } A \sim 0.1$$

For quartz this leads to a minimum grain radius for detachment of about 40 μm when $u^* \geq 20$ cms^{-1}. It follows that grains smaller than this are not readily raised from the surface. They may, however, be detached by saltation. Once large grains begin to move they collide with surface obstructions and bounce into the air; these collisions can then detach and project smaller particles. The size of silicate particles found over the Atlantic in air blown off the Sahara ranged typically between 0.3 and 20 μm radius, with a mode near 2 to 5 μm. (Prospero and Carlson, 1972).

In passing, it is worth noting that there is a limit to the extent to which solids can be reduced in size by mechanical forces; whether these are natural, as in a volcanic eruption or man made as in milling, crushing or explosive processes. Thus if material is ground for an indefinite period, after a certain time no changes in the particle size distribution is apparent. A plausible explanation for this observation is that while particles of all sizes are broken down, some particles, probably the smallest ones, unite with one another or with larger particles as rapidly as they are formed. Such adhesion is attributed in part to the action of the weak London - van der Waal forces of attraction which exist between all molecules. These have the form:

$$F = 4 10^{-14} \frac{d}{x^2} \text{ dynes for two solid particles of diameters}$$

d where x is the separation (assumed to be $3_{10}-8$ cm when the spheres are in contact). For adhesion one might equate this force to the

weight of either particle, ie $d^2 \leq 4\,10^{-17}/x^2$ for $\rho \sim 2 g/cm^3$. Even for $x \sim 10^{-6}$cm, particles up to 30 μm radius can be expected to adhere. Of course the problem of bringing such particles together is not a trivial one and will be returned to in subsequent lectures.

3.2 Formation of particles at liquid surfaces

Atomizers, sprays and other such devices have a common principle of operation. The liquid is drawn out into threads or sheets, usually under the shearing action of an air stream; these in turn collapse into fragments the size of which is determined principally by the thickness of the film. Monk (1952) calculated that $2\,10^6$ cal sec^{-1} would be required to 'atomize' a liquid by pulling it down to 1 μm threads at a rate of 1 cm^3 per second. The production of micron or less sized drops by such methods is therefore difficult and inefficient.

A much more important mechanism for the atmosphere is the bursting of bubbles at the ocean surface. This process has been thoroughly investigated by Woodcock (1953), Blanchard (1967) and others. They have shown that each air bubble which reaches the surface develops a spherical cap which drains, thins and then bursts. Fragments of the film cap are thrown upward by air escaping from the bubble orifice. Now deprived of its cap, the bubble fills with water rushing down the sides of the cavity, which subsequently emerges from the centre as a narrow jet. As the jet rises it becomes unstable and eventually disintigrates into a few large and several small drops. The sea salt 'giant' aerosol reported earlier from Woodcock's results are believed to originate almost exclusively from the jet drops. Bubbles of 2 mm diameter project drops to a height of nearly 18 cm above the ocean surface, and are of course responsible for the effervescence of carbonated drinks.

An interesting suggestion that the collapse of the bubble walls to form the jet, shears off a very thin layer from the surface of the bubble (~ 0.5 μm for a 1 mm bubble) has been made by MacIntyre (1974). This could have the effect of concentrating the long chain molecules that form a ubiquitous coat on the surface of liquids. Lipids, such as soap, are a common example having a hydrophobic tail and hydrophilic head. They are known as surfactants because of their modification of surface properties. Subsequent evaporation of the jet drops to form aerosol, of perhaps fractionated sea salt and a concentration of surfactants, would have some interesting properties. Bubbles of diameter 2 mm are known to produce dry particles, predominantly of salt, of about 25 μm radius from this jet; 100 μm and 20 μm bubbles produce dry particles of about 1.3 μm and 0.3 μm respectively. Smaller bubbles rapidly disolve in the surrounding liquid and have a low rate of rise. Again this is compatible with the observed low size limit of the sea salt aerosol.

Blanchard (1967) has estimated that about 10^{18} to 10^{20} sec^{-1} bubbles burst at the ocean surface, on average. This creates a mass flux of sea salt amounting to 10^3 to 10^4 megatons per year; a figure comparable with industrial emissions.

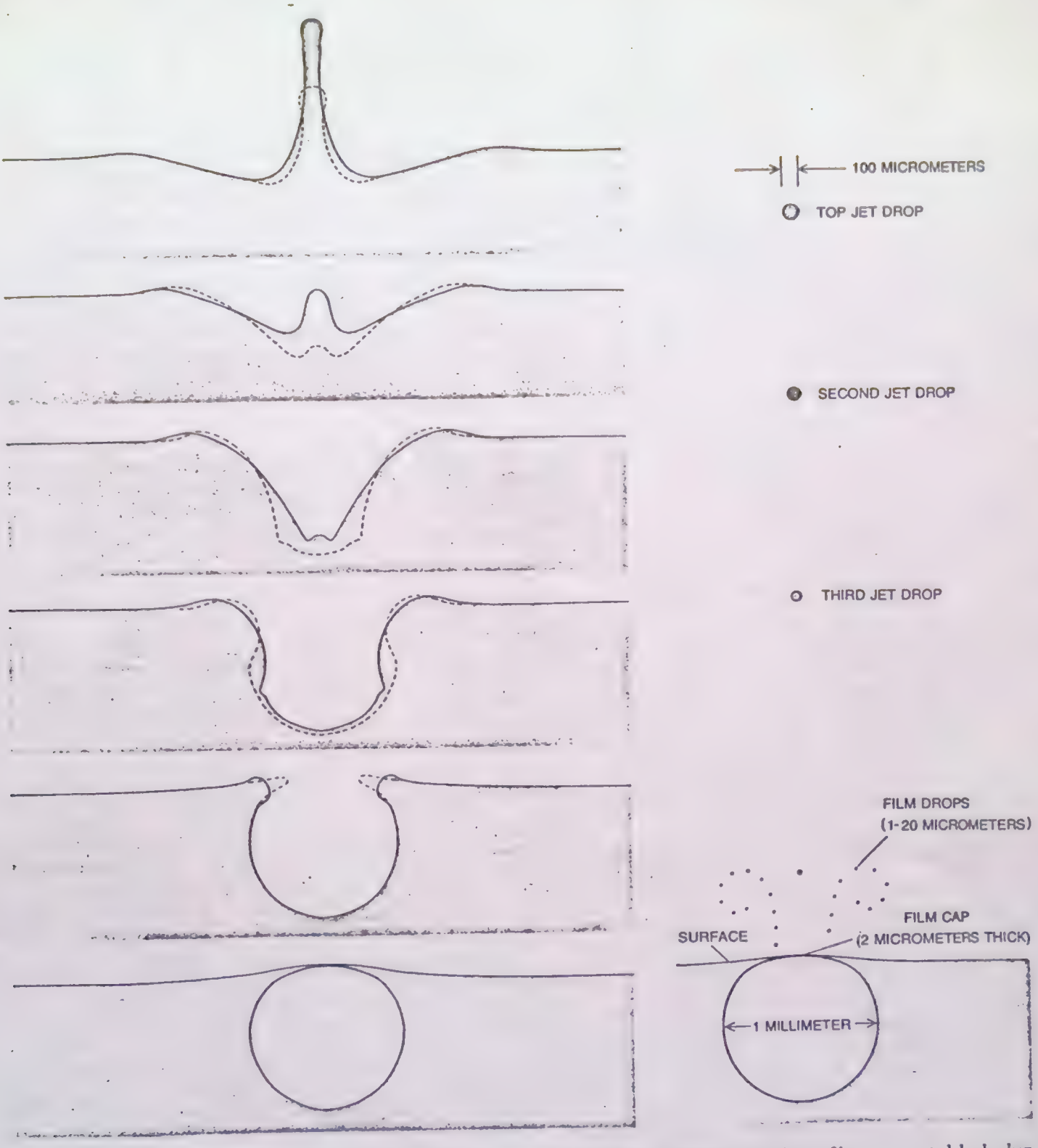

BREAKING BUBBLES, according to the author's hypothesis, provide the chief mechanism for injecting into the atmosphere a peculiar selection of the substances present in the top micrometer of the ocean. The six drawings at the left show how a collapsing bubble projects a high-velocity jet of liquid into the air. The sequence is based on high-speed photographs of a 1.7-millimeter bubble made by Duncan C. Blanchard, A. H. Woodcock and others at the Woods Hole Oceanographic Institution. The drawings depict the collapse at intervals of 1/3,000th second; profiles represented by broken lines show an intermediate stage 1/6,000th second earlier. The acceleration of surface material can reach 1,000 times gravity (1,000 *g*) for a 1.7-millimeter bubble and as much as a million *g* for a 10-micrometer bubble. The drawing at right shows schematically the variety of drops produced by a bursting bubble. Roughly a fourth of the available energy is carried off by the top drop of the jet, which then frequently evaporates into an airborne particle of salt.

This diagram is taken from 'Scientific American'
May 1974.

3.3 Formation of new particles from the gas phase

The molecules of a vapour make frequent encounters with each other and have ample opportunity to become associated into groupings of more than one molecule - dimers, trimers etc - which may exist for a time before being broken up into smaller fragments or completely back to unassociated molecules. By Boltzmann statisitics the number of embryos of a given size is proportional to $\exp(-\Delta G/KT)$ where ΔG is the free energy associated with a specific embryo. Molecules of any arbitary grouping of molecules possess potential and kinetic energy. In principle it is possible to set up the equations of motion and evaluate the eigenvalues. In practice, this is impossible in all but the simplest cases. The problem can be overcome by gross simplification; typically using what is known as the 'liquid drop model'. Its particular features are that the free energy of a grouping of n molecules is reduced to a sum of two terms; one proportional to volume or n and another to surface area, or $n^{\frac{2}{3}}$. Effectively the huge numbers of positions which a molecule can assume is reduced to three: an interior position in which the molecule is subject to balanced intermolecular forces; a surface position to which the molecule can be moved from the interior only by doing work against the intermolecular forces; and a 'free' vapour position.

The expression for ΔG is evaluated by analogy with the classical concept of a macroscopic liquid drop. The surface energy term is simply $4\pi r^2\sigma$ where σ is the surface free energy per unit area, or surface tension. The volume term is evaluated by recognising that vapour at saturation is in equilibrium with the bulk phase. The free energy of a molecule in the condensed phase can then be equated to the free energy of a molecule in the vapour at saturation. The work done by the vapour in compressing or expanding isothermally from e to es is then equal to the free energy excess. For one molecule this work is $KT \ln(e/es)$, or $RT \ln(e/es)$ per mole. The fractional extent to which e exceeds es is called the supersaturation, ie $S = e/es - 1$.

Thus $$\Delta G = -\frac{4}{3}\pi r^3 \frac{\rho}{M} RT \ln(1+S) + 4\pi r^2\sigma$$

This has the form $\Delta G = \alpha r^3 + \beta r^2$ which varies with r as shown below.

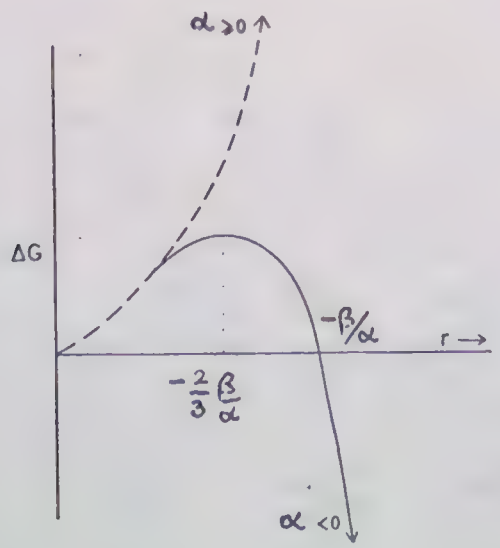

i. Variation with size of the free energy ΔG of an embryo of condensate.

where $\alpha = -\frac{4\pi}{3}\frac{\rho}{M} RT \ln(1+S)$ and $\beta = 4\pi\sigma$

$\frac{d\Delta G}{dr} = 0$ when $r = 2\beta/3\alpha$. This occurs only if $\beta/\alpha < 0$

or $s > 1$. Then a critical radius and embryo energy can be defined

$$r^* = \frac{2\sigma M}{\rho RT \ln(1+S)}, \qquad \Delta G^* = \frac{16\pi\sigma^3 M^2}{3\rho^2 R^2 T^2} \frac{1}{[\ln(1+S)]^2}$$

For water (σ = 76 erg cm^{-2}, M = 18)

r^* (cm) = $1.1\ 10^{-7}/\ln(1+S) \simeq 1.1\ 10^{-7}/S$ for $S \ll 1$

Hence at small supersaturations (say $0.1\% < S < 1\%$) $r^* \sim 10^{-1}$ to 10^{-2} μm.
At large supersaturations - say S $\sim$ 200%, $r^* \sim 10^{-3}\mu$m.
The rate of homogenous nucleation is simply the rate at wh ch supercritical embryos are formed, and is given by the product of the concentration of embryos and the rate at which a critical drop gains another molecule and becomes supercritical;

$$J = 4\pi r^{*2} \frac{e}{\sqrt{2\pi m kT}} Z n \exp\left(-\frac{4\pi r^{*2}\sigma}{3kT}\right)$$

where m is the mass of the water molecule, n is the number density of vapour molecules and Z is a factor $\sim$ 0.01. By substituting for r* in terms of S, the rate of homogenous nucleation as a function of S can be calculated. Because of the exponential term, the nucleation rate changes from vanishingly small to extremely large values over a very narrow range of S. The value of S for which this occurs is called the critical supersaturation Sc, and by convention corresponds to J = 1 cm^{-3} sec^{-1}. It is found that Sc $\simeq$ 3.2 at +3°C and Sc=5 at -12°C, for water. Such large supersaturations are never observed in the atmosphere and so homogenous nucleation of liquid water from its vapour is of no practical importance. For molecules other than water, it is not certain what mechanisms or reactions can lead to vapour supersaturations capable of driving homogenous nucleation. Furthermore it is not easy to see why such nucleation should occur in the presence of already existing particles, for example . However it is almost certain that a large proportion (numerically) of natural aerosol particles are produced in this way. The difficulty of the problem may be appreciated by considering the nucleation of aqueous sulphuric acid in an atmosphere containing H_2SO_4 vapour and water vapour. Embryos may exist with a variety of proportions of sulphuric acid and water. The 2 dimensional diagram relating ΔG to r now becomes 3 dimensional relating ΔG, r and say mole fraction. (See the diagram on the next page). Particle formation can proceed from very small radii to large radii by an infinity of paths, in which some maximum ΔG is experienced. This governs the nucleation rate for the path and the saddle point defines that which is energetically preferred.

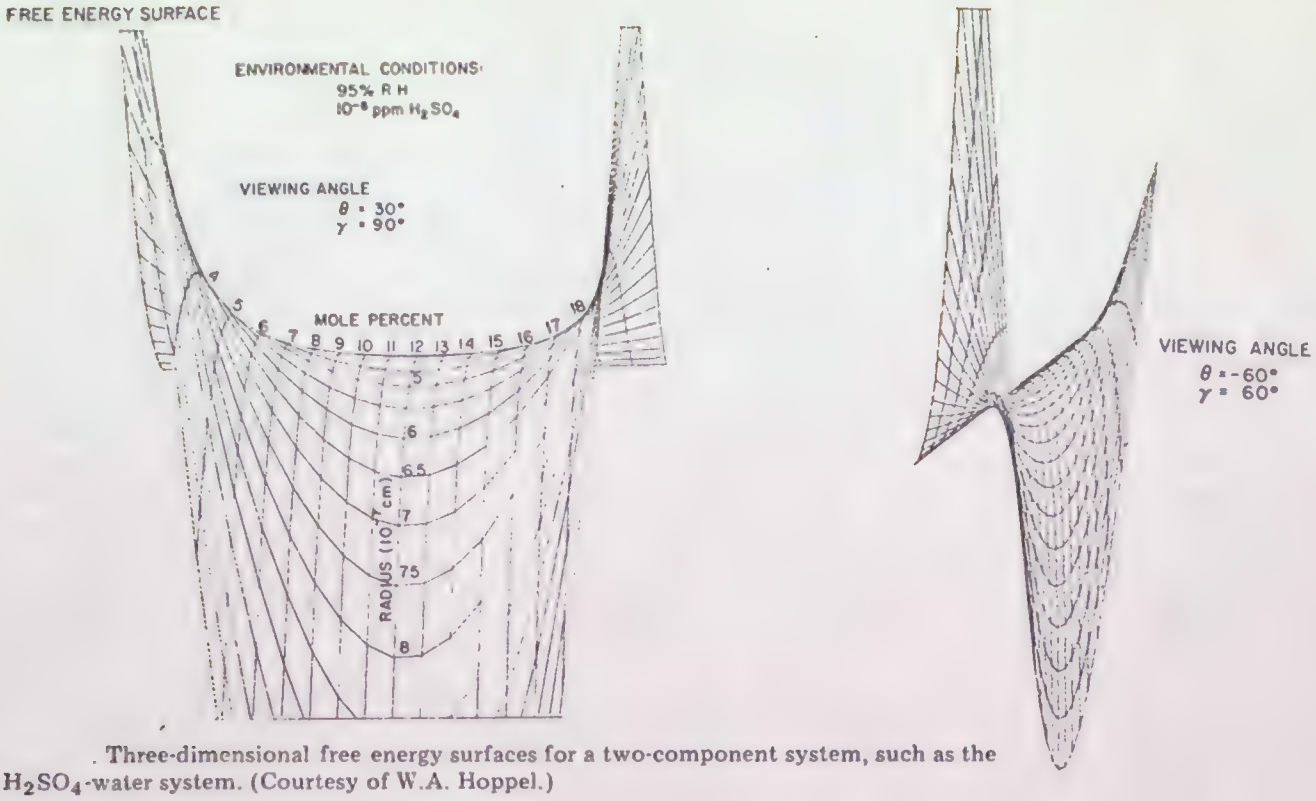

. Three-dimensional free energy surfaces for a two-component system, such as the H_2SO_4-water system. (Courtesy of W.A. Hoppel.)

3.4 Condensation growth of wet aerosol

Although the role of supersaturation has been identified as an important 'driving force' for particle formation and growth, it is apparent above that the energetics of the processes as described so far are unfavourable for the initial condensation of water vapour in the real atmosphere. Obviously physical processes which reduce ΔG provide a way of overcoming this difficulty. The necessary invocation of external influences has lead to the term heterogenous nucleation

(a) if an electric charge term is included in ΔG it becomes

$$\Delta G = -\frac{4}{3}\pi r^3 \frac{\rho}{M} RT \ln(1+S) + 4\pi r^2\sigma + \frac{1}{2}q^2\left(1-\frac{1}{\varepsilon}\right)\left(\frac{1}{r}-\frac{1}{r_{ion}}\right)$$

For unit charge the additional term has only a small effect in reducing ΔG^* so that at ambient temperature the critical supersaturations is reduced to about 200%.

(b) Condensation on an insoluble particle is conceptually attractive. If the particle is perfectly wetted by the water, (so that it can be considered energetically as being formed of water) then as before for small supersaturations,

$$S_c = 1.1\,10^{-7}/r_c$$

and for a critical supersaturation of 1% a critical embryo is formed by a particle of radius $\sim 0.1\ \mu m$. The difficulty derives from the high surface energy of water; few common insoluble materials have the necessary much greater surface energy to produce a small contact angle. On non wetting substrates small drops have to form – and as we have seen these are not capable of being produced at an appreciable rate by normal atmospheric supersaturations.

(c) A dissolved solute tends to lower the equilibrium vapour pressure of a liquid. Physically one may imagine that some of the molecules that were in the surface layer are replaced by solute molecules. If, as is usually the case when the liquid is water, the vapour pressure of the solute is less that that of the liquid, the effective vapour pressure is reduced in proportion to the amount present. The reduction in vapour pressure due to the presence of a solute may be expressed as:

$$\frac{e'_s}{e_s} = \frac{n_o}{n + n_o}$$

where the solution consists of n_o molecules of water and n molecules of solute. This is known as Raoult's Law. For dilute solutions

$$\frac{e'_s}{e_s} = 1 - \frac{n}{n_o}$$

For solutions in which the dissolved molecules are dissociated the above expression must be modified by multiplying n by a factor i – the degree of ionic dissociation. (Recall that many substances in small quantities dissociate almost completely in water). The number i is is known as the Van't Hoff factor; for NaCl i=2, for $(NH_4)_2SO_4$ i=3 to a good degree of approximation, although strictly i should be evaluated as a function of solute concentration.

$$\text{Thus} \quad n = i N_A \frac{M}{m_s} \quad \text{and} \quad n_o = N_A \frac{m}{m_w}$$

where N_A is Avogardro's number, M and m are the mass of solute and water respectively; m_s and m_w are their molecular weights. Writing

$$m = \frac{4}{3}\pi r^3 \rho_w$$

$$\frac{e'_s}{e_s} = 1 - \frac{b}{r^3} \quad \text{where} \quad b = \frac{3 i m_w M}{4\pi \rho_w m_s}$$

e_s represents the vapour pressure of a pure water drop of radius r. To relate this to the saturation vapour pressure over a flat surface,

$$\frac{e'_s(r)}{e_s(\infty)} = \left(1 - \frac{b}{r^3}\right) \exp\left(\frac{2\sigma M}{\rho_s R T r}\right)$$

The assumptions made – a relatively dilute solution and a reasonably large droplet – require that b/r^3 and $\frac{2\sigma M}{\rho_s R T r}$ are small,

so that the most commonly used form of the equation is

$$S_o = \frac{e'_s(r)}{e_s(\infty)} - 1 = \frac{a}{r} - \frac{b}{r^3}$$

where S_o is the equilibrium supersaturation for a given amount and type of solute. Note that this equilibrium supersaturation may be negative (ie RH < 100%) for some combinations. The resulting graphical representations of these equilibrium states are known as Kohler curves.

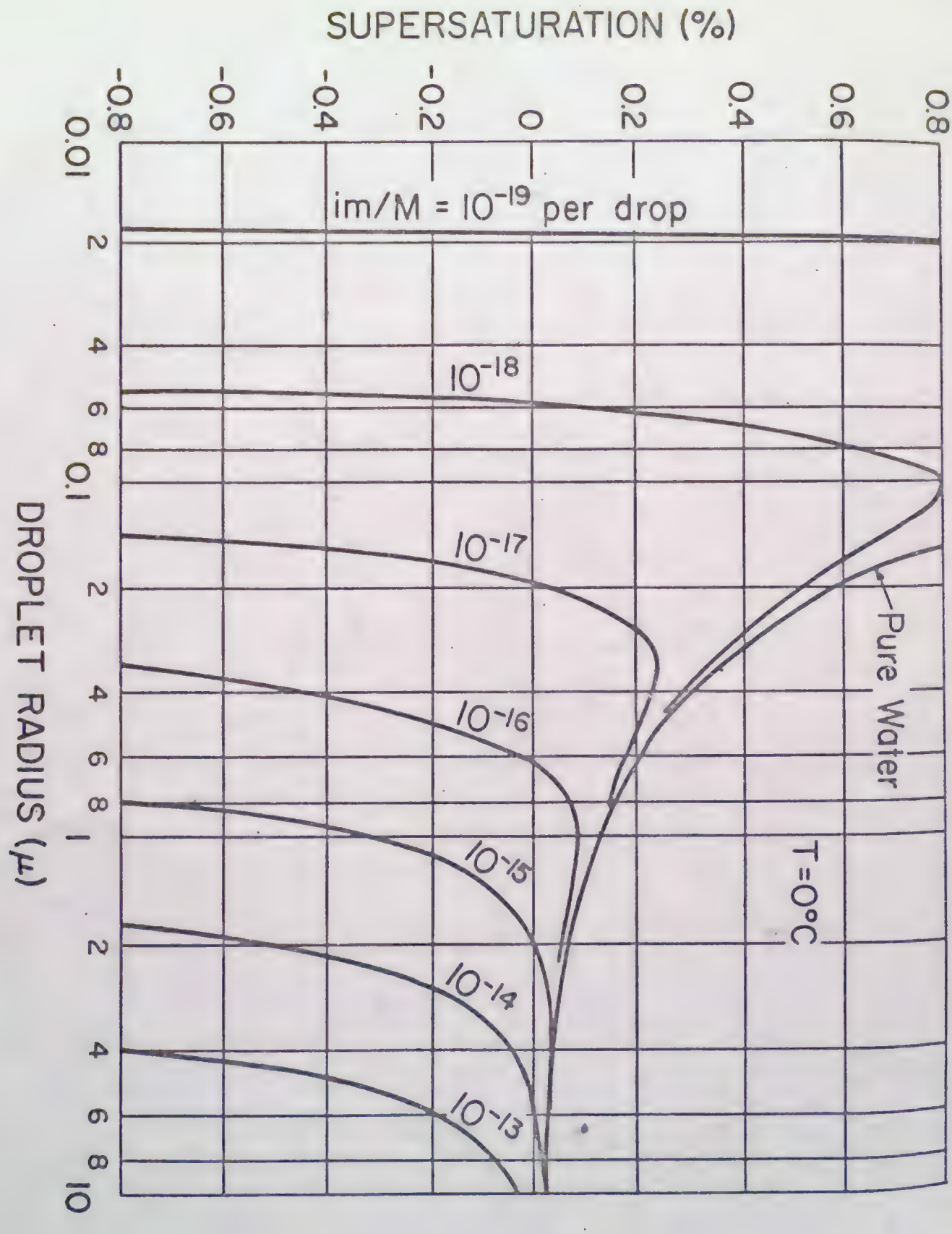
SUPERSATURATION (%)
-0.8
-0.6
-0.4
-0.2
0
0.2
0.4
0.6
0.8
im/M = 10^-19 per drop
10^-18
10^-17
10^-16
10^-15
10^-14
10^-13
Pure Water
T=0°C
DROPLET RADIUS (μ)
0.01
2
4
6
8
0.1
2
4
6
8
1
2
4
6
8
10

The significance of the maxima in these curves is that up to this point it is necessary for the relative humidity to increase to allow a drop in equilibrium to grow. Once the point is reached, growth will continue without additional increase in relative humidity. Whether or not it will do so, or the relative humidity will be drawn down, depends on the water substance budget. Intuitively, however we might expect that a supersaturation maximum will occur close to a cloud boundary and only particles with their critical supersaturations less than this maximum will participate actively in further condensational growth. The others remain unactivated; ie to the left of their Köhler curve maxima.

Once activated the growth of the drop is driven by the difference between the environmental vapour pressure and the equilibrium value. The following growth equation results

$$r\frac{dr}{dt} = C\left(S - \frac{a}{r} + \frac{b}{r^3}\right)$$

where C is a function of the rates at which heat (released as latent heat of condensation) is conducted away from the drop and water vapour is diffused to the drop. The details of this will be discussed in the discussion on scavenging but for the present it is sufficient to note that C is a function of pressure and temperature only.

After r becomes sufficiently large a/r and b/r^3 are negligible and to a good approximation

$$r\frac{dr}{dt} = CS$$

Thus a droplet experiencing constant supersaturation is predicted to grow as

$$r(t) = \sqrt{r_0^2 + 2CSt}$$

In round figures $r_0^2 - r_t^2 = 120St$ if r is in μm and t in seconds. The parabolic form of this growth law predicts that a distribution of drops should become narrower as growth proceeds; that in general, it does not, is discussed in subsequent lectures!

In natural clouds many droplets grow at the same time and compete for the available water vapour. If moisture is supplied by saturated air which is cooled in ascent (and there <u>are</u> other ways of releasing moisture)

$$\Delta S = \left(\frac{g M_\omega L}{RT^2 C_p} - g\frac{M_A}{RT}\right)\Delta z - \left(\frac{1}{\rho_s} + \frac{M_\omega L^2}{C_p p M_A T}\right)\Delta W$$

Where ρ_s is the saturation vapour density
M_ω is the molecular weight of water
M_A is the molecular weight of air
L, T, g and R have their usualmeaning

This expression simply identifies the supersaturation change as the difference between a production term due to ascent, Δz and a loss term $\Delta\omega$, the mass of water condensed.
To close the equation $\Delta\omega$ and ΔS must be separately related through the droplet growth equation. viz

$$\Delta\omega = 4\pi r^2 \rho_L \Delta r$$
$$r\Delta r = CS\Delta t$$
$$\Delta\omega = 4\pi r \rho_L CS\Delta t$$

By summing over all drops in the volume: $\frac{dS}{dt} = \alpha V - \beta S \Sigma r$

Typically $\alpha = 6 \times 10^{-6}$ cm^{-1}, $\beta = 3$ cm^{-1}s^{-1} $\quad G = 6 \times 10^{-7}$ cm^{2}s^{-1}

Thus (a) in the absence of condensation, relative humidity in a rising air parcel increases at about 6% per 100 m.

(b) instantaneously, an updraught of about 2.5 ms^{-1} is capable of maintaining a constant supersaturation of 0.5% in the presence of 100 drops per cc of mean radius 10 um. Such drops grow at a rate of about 2 um per min under these conditions.

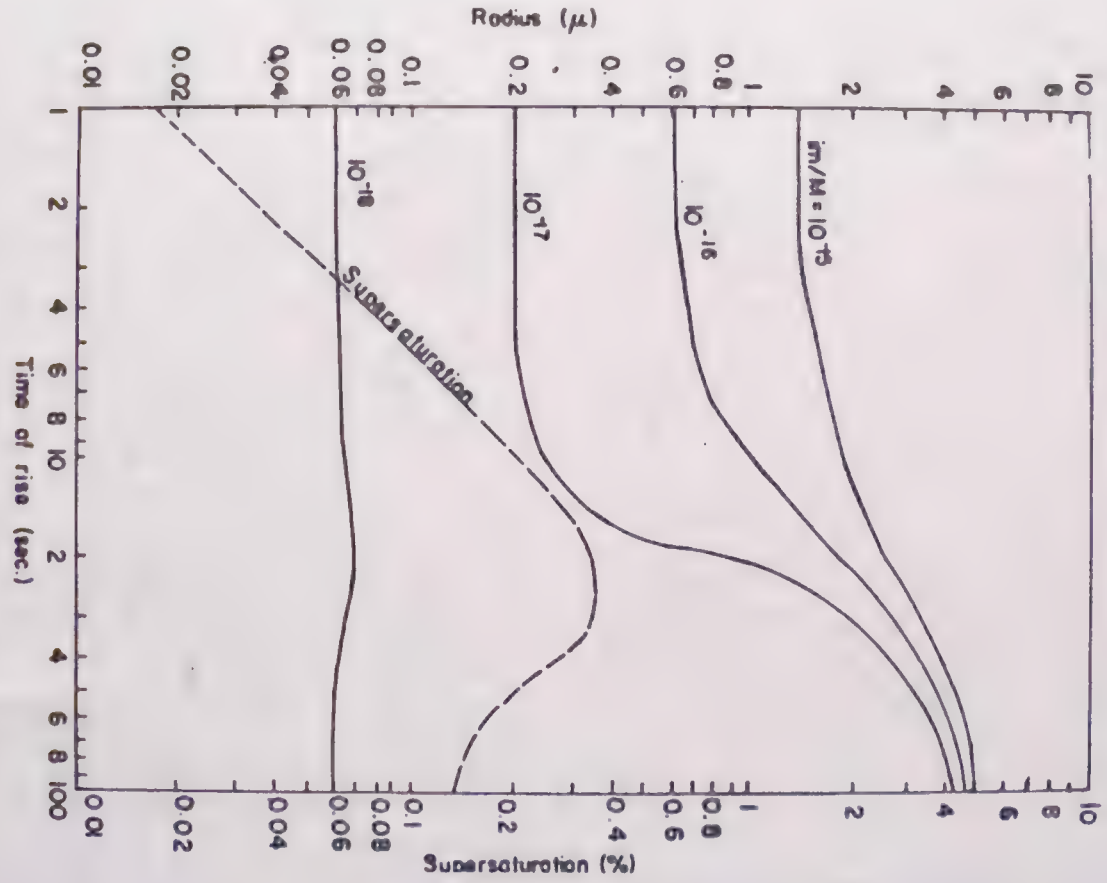

The figure above shows the growth of droplets by condensation onto various masses of salt in an updraught of velocity 0.6 ms^{-1}. The calculations show that

(a) For the first 10 seconds, when the rate of condensation is negligible the supersaturation increases linearly with time. It reached a maximum of 0.35% in 25 sec and then decreases.

(b) Above a certain critical supersaturation, the droplets grow rapidly and tend to a uniform size.

(c) As the supersaturation falls, the smaller drops which have not been activated fall back to smaller sizes but large drops continue to grow rapidly.

(d) Growth by condensation becomes very slow after a few minutes and drops have only reached a radius of about 20 μm in 10 minutes.

References

Bagnold, R A, 1941: The Physics of Blown Sand and Desert Dunes, Methuen

Best, A C, 1951: Quart. J. Roy. Meteor. Soc., 77, 418

Blanchard, D C, 1967: From raindrops to Volcanoes: Adventures in Sea Surface Meteorology, Doubleday.

*Junge, C E, 1963: Air Chemistry and Radioactivity, Academic Press

MacIntyre, F, 1974: Sci. Amer (May), 62

*Mason, B J, 1971: The Physics of Clouds, Oxford

Monk, G W, 1952: J. Appl. Phys. 23, 288

Prospero, J M & T N Carlson, 1972: J Geophys. Res, 77, 5225

*Pruppacher, H R & Klett, J D, 1978: Microphysics of Clouds and Precipitation, D Reidel

*Rogers, R R, 1976: A Short Course in Cloud Physics, Pergamon

*Twomey, S, 1977: Atmospheric Aerosols, Elsevier

Woodcock, A H, 1953: J Meteorol., 10, 362

* Particularly usefule general reference works.

METEOROLOGICAL OFFICE
4 JUL 1990
LIBRARY

An Introduction to Cloud Microphysics (2)

by P Ryder

4 Growth of precipitation particles by coalescence

The relative sizes of cloud and raindrops are shown below. The volume of a typical cloud droplet ($r = 10\mu m$) has to increase by 10^6 in order to produce a precipitable particle of radius 1 mm. Condensation alone is too slow a process to achieve such growth. In warm clouds precipitable drops can only form by the collision and coalescence of cloud droplets of different sizes.

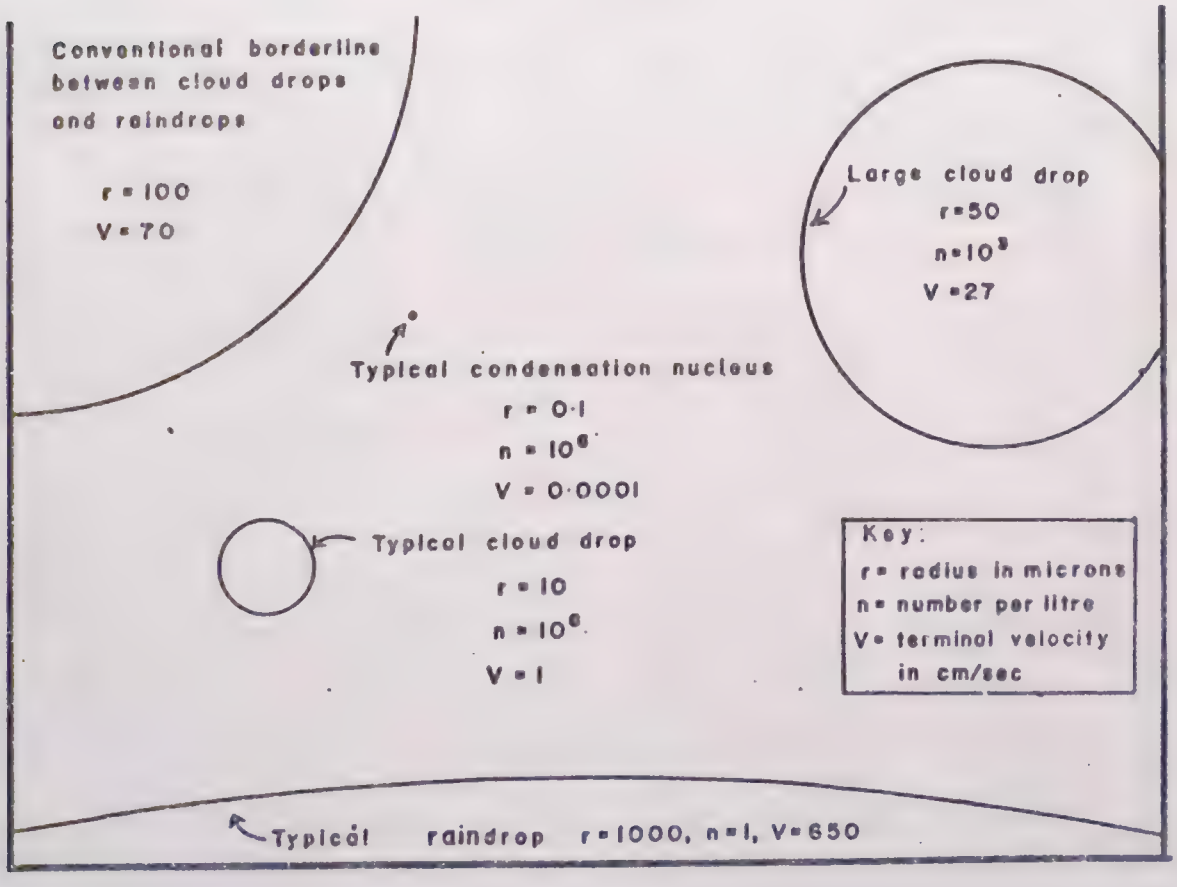

The details of how the necessary spread in droplet sizes is (or is not) achieved will be discussed in subsequent lectures. Here we restrict attention to the essential physics of the coalescence process.

An incipient raindrop of radius R and terminal velocity V_R may, in falling through a cloud, overtake and collide with a smaller droplet of radius r and terminal velocity v_r as shown below.

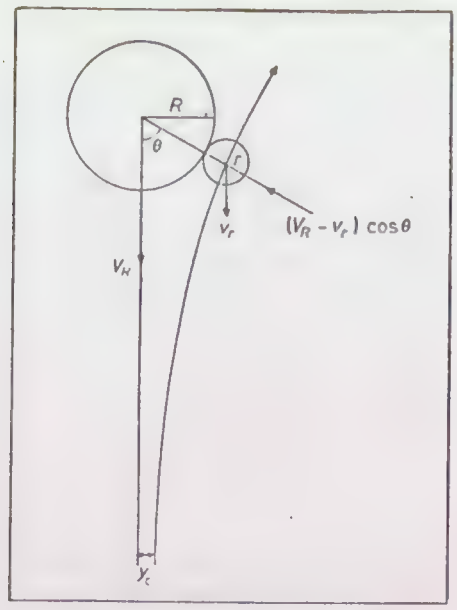

Relative trajectory of a small droplet colliding with a larger overtaking drop

A droplet being overtaken by a larger drop in still air will, when the vertical separation is large, approach the latter along a straight line path at velocity $V_R - V_r$ but as they come closer together the smaller drop will tend to follow the airflow round the larger. A tiny droplet with negligible inertia will follow the streamlines and miss the larger drop altogether. A larger droplet may have sufficient inertia to deviate from the streamlines and collide with the drop. Whether the two will collide is a function of their sizes, the initial relative trajectory and the kinematic viscosity of the air.

We define the collision efficiency E as the fraction of droplets within the geometrical cross-section of a collector drop which actually collide with the collector

Thus $$E = y_c^2/(R+r)^2$$

The average growth rate of the drop by collision and coalescence with droplets of radius r and spatial concentration n_r is

$$\frac{dM_R}{dt} = 4\pi\rho_L R^2 \frac{dR}{dt} = E_2 \pi y_c^2 (V_R - v_r)\left(\frac{4}{3}\pi n_r \rho_L r^3\right)$$

$$\text{or} \quad \frac{dR}{dt} = \frac{E_1 E_2}{4}\left(\frac{R+r}{R}\right)^2 (V_R - v_r)\left(\frac{4}{3}\pi n_r \rho_L r^3\right)$$

where E_2 is defined as the coalescence efficiency, the fraction of colliding droplets that coalesce. The product of E_1 and E_2 is often known as the collection efficiency.

No general solution to the equations of motion of two liquid spheres including both inertial and viscous terms and fluid motion within and outside the drops has been found, but solutions for some combinations of the various parameters are shown below.

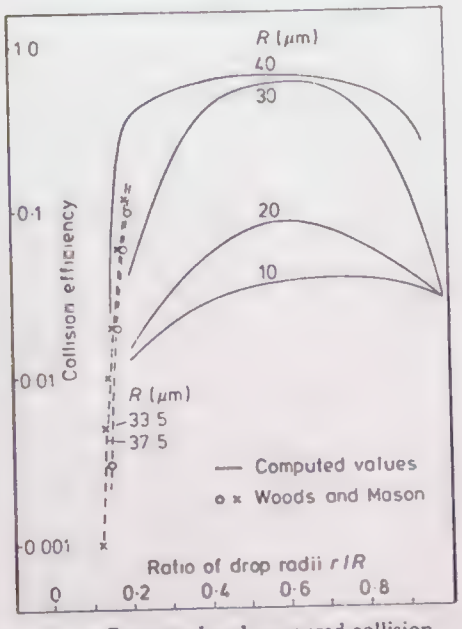

Computed and measured collision efficiencies of small droplets

Computed and measured collision efficiencies for drops of radius 40–80 μm colliding with smaller droplets (— computed values, – – experimental results, •o Woods and Mason, ×Picknett, ▲ Beard and Pruppacher)

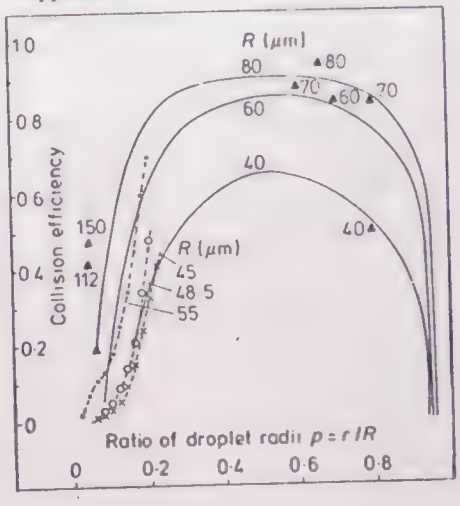

A number of essential features can be identified.

(a) The larger the collector drop the higher the collision efficiency.
(b) The collision efficiency is very small but still finite when the radius of the collector drop falls below 20 μm
(c) The probability of collision is very small for small collected drops

It is known that under certain conditions (not necessarily representative of those in the atmosphere) droplets can rebound after colliding with a water surface. However it is generally assumed that in natural clouds the coalescence efficiency E_2 is unity.

The growth equation given above can be used in an appropriate dynamical framework to calculate the growth of a raindrop falling through a uniform cloud of known liquid water content. Such a model predicts that all drops of a given size grow at the same rate. The results establish associations amongst updraught, cloud height, time for rain production and the size of drops produced, that are in qualitative accord with observations. The most serious discrepancy between model predictions and observations lies in the time requirement; large drops appear too late in the model by about a factor of two.

A solution to this dilemma can be found when it is recognised that there will be local variations in the concentration of drops in a volume. The growth equation does not take the statistical fluctuations into account; it is not the average growth that figures in the development of rain. Some statistically 'fortunate' drops fall through regions of high concentration sweeping up more than the average liquid water and are subsequently in a favoured position to continue to grow rapidly. This stochastic concept

is particularly important in the early stages; typically the first twenty captures. A schematic of the first two such events is shown below when some 10% of drops experience enhanced growth.

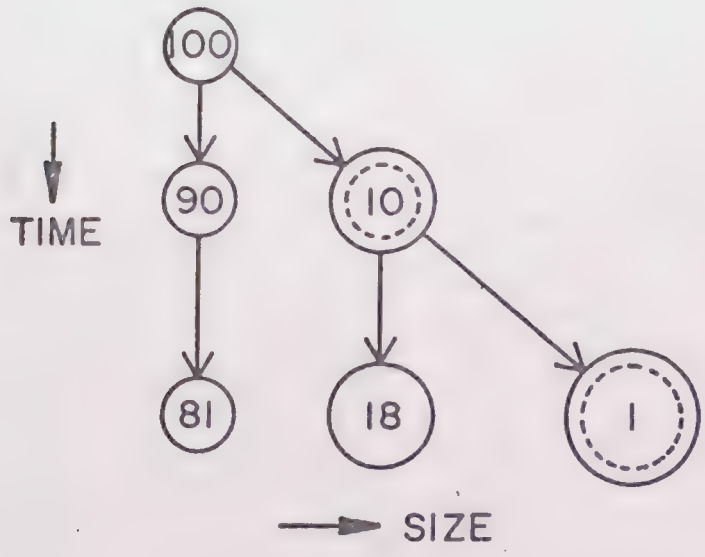

The equation expressing the coagulation process must now take the entire droplet spectrum into consideration. In general it will have the form

$$\frac{dn(v)}{dt} = -n(v)\int_0^\infty K(v,u)\,n(u)\,du + \frac{1}{2}\int_0^v K(v-u,u)\,n(v-u)\,n(u)\,du$$

a loss term due to collisions between drops of mass v with all others

a production term involving collisions between drops smaller than v, which when they coalesce form a drop of v

Here $K(r_1^3, r_2^3)$ is the so called coagulation kernel given by:

$$K(r_1^3, r_2^3) = E_1(r_1, r_2)\,E_2(r_1, r_2)\,\pi\,(r_1 + r_2)^2\,\left|V(r_1) - V(r_2)\right|$$

and V (r) is the terminal velocity of the drop of radius r .

This kernel increases rapidly with increasing droplet size and leads to a positive feedback effect for the favoured few. A number of authors have developed models based on these ideas, including the effects of fluctuations in the n(u). These studies and their results are

reviewed in chapter 15 of Pruppacher and Klett (1978). The figure below, from Berry and Reinhardt (1974), shows a typical evolution.

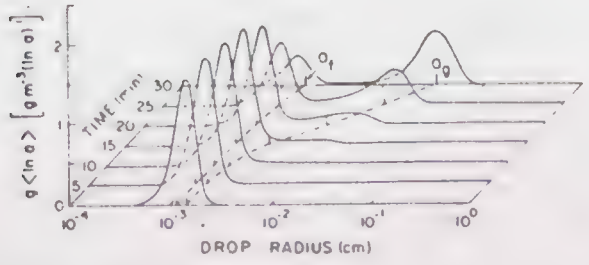

Time evolution of the liquid water spectrum: $a_f(0) = 12\,\mu$m, var x = 1. (From Berry and Reinhardt, 1974c; by courtesy of Amer. Meteor. Soc., and the authors.)

Several authors have attempted to parameterise this process (which is difficult and expensive to evaluate in full). The result of Berry (1968) captures the essential physics.

$$\text{Thus} \quad \frac{dM}{dt} = \frac{\omega^2}{60(2+0.0266\,N_0/\beta)}$$

where the conversion of cloud water to precipitation sizes (dM/dt) is related to cloud drop concentration N, the dispersion of the initial distribution β, and liquid water content of the cloud ω. In general dynamical processes and the supply of moisture control ω, but N_0/β is large in clouds formed in continental air but small in maritime clouds.

5 Initiation of the ice phase

Two phase transitions can lead to ice formation: the freezing of a liquid droplet or the direct deposition (sublimation) of vapour to the solid phase. In view of the previous discussion of the vapour–liquid transition it should come as no surprise that nucleation is necessary to overcome the surface free energy barrier of the solid/liquid or solid/vapour interface. Again both homogenous and heterogenous nucleation are possible.

In general the theory of ice nucleation has suffered from the difficulty of defining the interfacial free energies for the transitions. However it is clear that homogeneous freezing requires a substantial supercooling. Thus small drops $\sim 5\,\mu$m freeze spontaneously at a temperature of about -40°C. Larger droplets freeze at a slightly warmer temperature. Homogeneous nucleation by sublimation or direct deposition is predicted to occur only for extreme conditions of supersaturation (ie $S_{ice} > 20$ a few degrees below 0°C, $S_{ice} \simeq 8$ at $T = -62^\circ$C). Although these latter conditions do not occur in the atmosphere, natural clouds have been observed to contain liquid drops down to -40°C.

Therefore it is likely that homogeneous nucleation with respect to freezing does occur in the atmosphere.

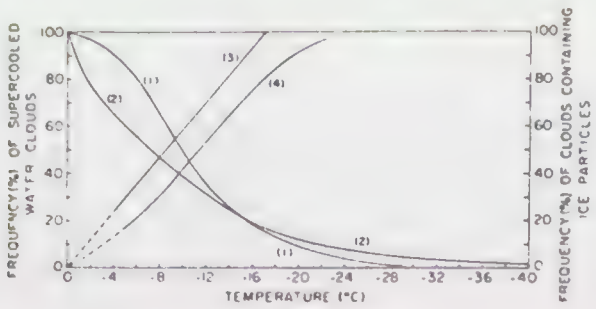

Variation of the frequency of supercooled clouds and of clouds containing ice crystals. Curves 1 and 2 pertain to ordinate at left. Curves 3 and 4 pertain to ordinate at right. (1) Peppler (1940), Germany, all water clouds; (2) Borovikov *et al.* (1963) ETU, all water clouds; (3) Mossop *et al.* (1970), Tasmania, mixed clouds; (4) Morris and Braham (1968), Minnesota, mixed clouds.

The appearance of ice crystals at temperatures considerably warmer than $-40^{\circ}C$ implies that heterogenous nucleation is occuring. It is found that the presence of a substrate reduces the surface free energy barrier. Intuitively it is expected that surfaces having a lattice structure similar to that of ice will be most effective. Silver iodide (AgI) possesses this property and is much used as an artificial ice nucleating agent – see the subsequent lecture on Weather Modification.

A nucleus may form an ice particle by

(a) direct deposition from the vapour. This can take place in the atmosphere provided ice saturation exists.

(b) condensation followed by freezing. This requires that the relative humidity exceeds that required for ice saturation and that of the phase transition point of a soluble nucleus. Thus in general this occurs at a higher relative humidity than (a).

(c) freezing of pre-existing cloud drops – so called contact nucleation.

In the atmosphere it is found that the concentration of ice nuclei is highly variable in space and time, but that a typical figure is 1 nucleus per litre at a temperature of $-20^{\circ}C$. The concentration usually depends strongly on temperature and as a rule of thumb a decrease of about $4^{\circ}C$ causes the concentration to increase by an order of magnitude. There can be wide deviations from the distribution shown.

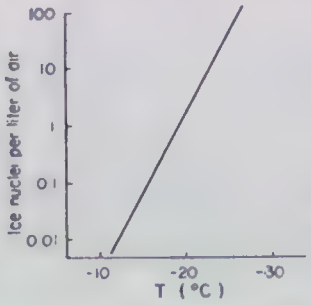

Typical dependence of ice nucleus concentration on temperature.

Since the probability of the occurrence of the ice phase in clouds increases with decreasing temperature, we might expect a monotonic rise in the concentration of such particles with decreasing temperature. This behaviour turns out to hold only in the minority of cases. More often a rapid phase change to ice occurs such that the ice particle concentration is not a function of further lowering of temperature.

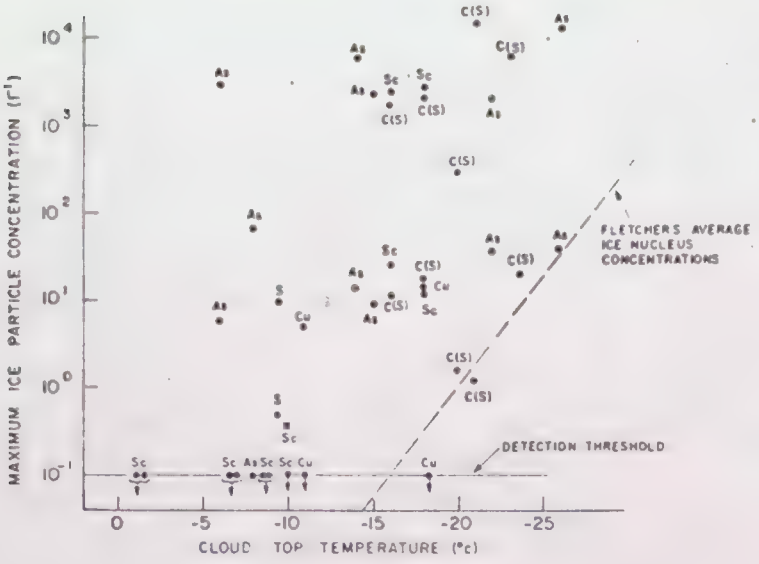

Hobbs et al (1974) summarised measurements in clouds over the Cascade Mts (Washington, USA). Little temperature sensitivity is discernable. The disparity between the number of ice nuclei and crystals is noteworthy.

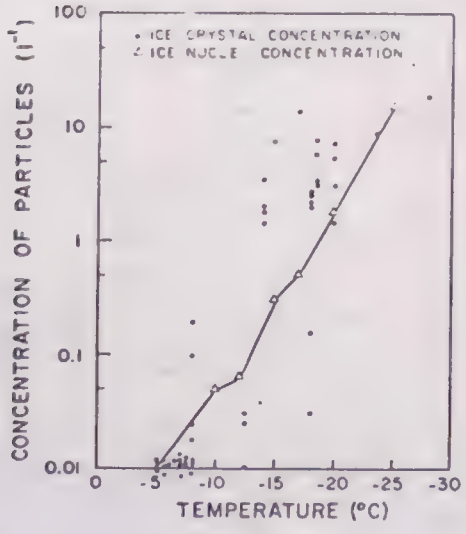

Gagin (1971) has shown that under some circumstances there is good agreement between the number of nuclei and ice crystals. The significance of these results will be discussed in the Weather Modification lecture.

An interesting recent development of unquantified relevance to the atmosphere has been the discovery that materials of biological origin may act as efficient ice nuclei - Schnell and Vali (1976). Thus nuclei active at temperatures as low as - 4°C have been found in decaying plant leaf litters; being a strong function of the climatic zone in which the litters were found. Active ice nuclei have been found in seawaters rich in phytoplankton. Vali et al (1976), Levin et al (1980) have also reported the existence of a few bacteria active as nuclei at relatively high temperatures (-2 to - 5°C). Again their atmospheric relevance remains obscure but they could be causative agents of frost damage in various plants, and therefore of considerable economic importance.

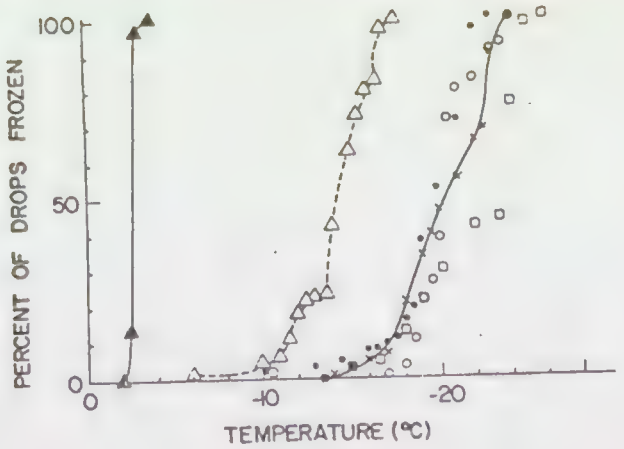

Fig. 2. Freezing temperature spectra of drops containing various ice nuclei, ▲ - M1 bacteria; •, O and □ - other yellow bacteria (named L1, L2 and L3 respectively) also isolated from citrus leaves. L1 cannot be distinguished from M1 by either colony morphology or substrate range; L2 differs from M1 with respect to substrate range; and L3 is distinguished from M1 by the fact that it forms rough colonies. x - saline (NaCl) solution. Δ - drops exposed to AgI aerosol particles.

Levin et al's data suggest that only a small proportion of the bacteria – rod shaped with a single polar flagellum – are active as condensation–freezing nuclei.

6 The form and growth of ice crystals

6.1 Crystal habits

Casual observation shows that ice crystals appear in a large variety of shapes or habits. More detailed studies show that from a crystallographic point of view, the crystals have the symmetry of a sixfold (hexagonal) prism. Laboratory experiments reveal that the rate of propagation of the basal faces (along the caxis) relative to the prism faces varies with temperature and supersaturation in a characteristic manner.

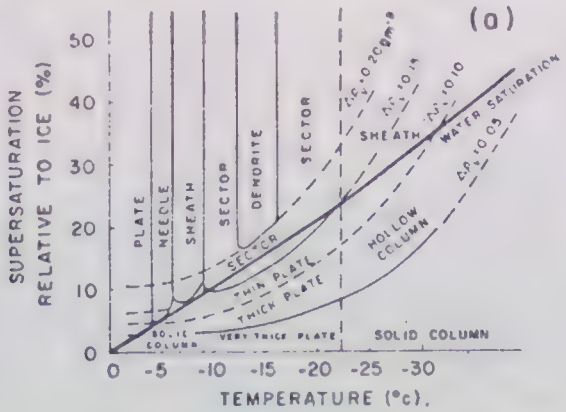

Variation of ice crystal habit with temperature and supersaturation. (Based on laboratory observations of Mason, 1971; Hallett and Mason, 1958; Kobayashi, 1961; and Weissweiler, 1969.)

Recall that significant supersaturations with respect to ice are produced for an ice crystal in the presence of water drops, because of the lower vapour pressure with respect to ice than water that exists at all temperatures below 0°C.

In the natural world pure crystal habits are rare. As a crystal experiences different environments of temperature and humidity growth habits become superimposed. Thus a columnar crystal suddenly surrounded by conditions which promote plate growth will develop end plates. Collisions between ice crystals and drops produce riming. Mogono and Lee (1966) have attempted a comprehensive classification of snow crystals which recognise these effects.

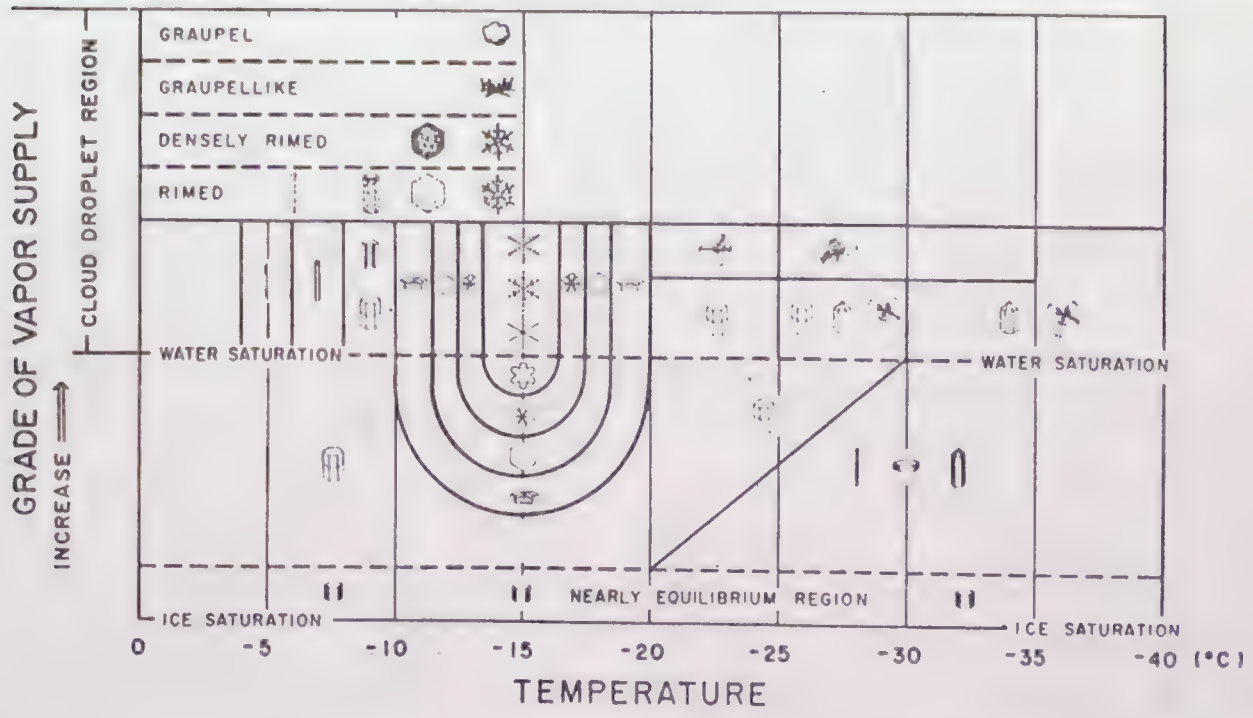

. Temperature and humidity conditions for the growth of natural snow crystals of various types. (From Magono and Lee, 1966;).

The size of a simple snow crystal can usually be characterised by two dimensions: the crystal diameter and thickness in the case of plate like crystals and crystal length and width for the columnar type.

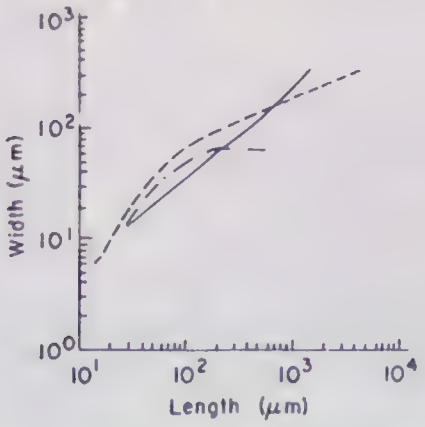

Dimensions of warm region ice columns observed in clouds. -·- Ono (1969), - - - Auer and Veal (1970), —— Hobbs *et al.* (1974a). (From Hobbs *et al.*, 1974a;

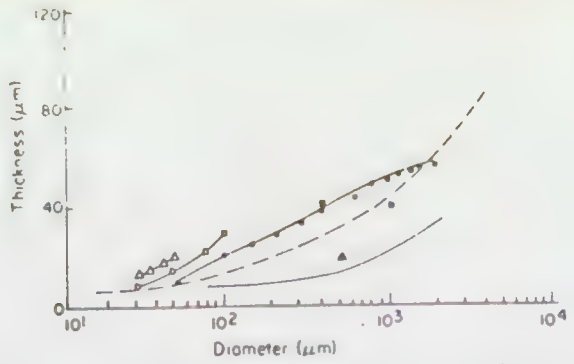

Dimensions of hexagonal ice plates observed in clouds. ■ Schaefer (1947), ▲ Weickmann (1949), □ Reynolds (1952), △ Mason (1953), ● Ono (1969), – – – Auer and Veal (1970), —— Hobbs *et al.* (1974a). (From Hobbs *et al.*, 1974a)

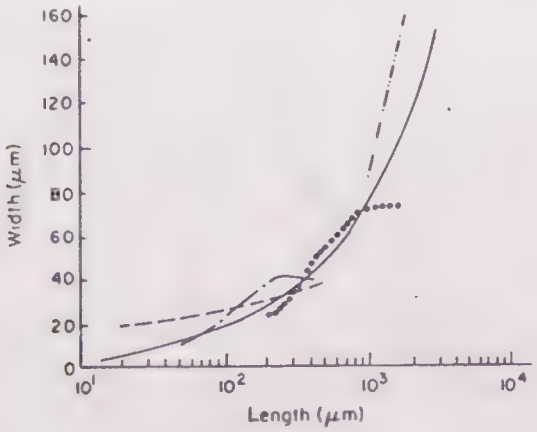

Dimensions of ice needles observed in clouds. –·– Magono (1954), – – – Isono (1959), –·– Ono (1969), —— Auer and Veal (1970), ○○○○ Hobbs *et al.* (1974a). (From Hobbs *et al.*, 1974a)

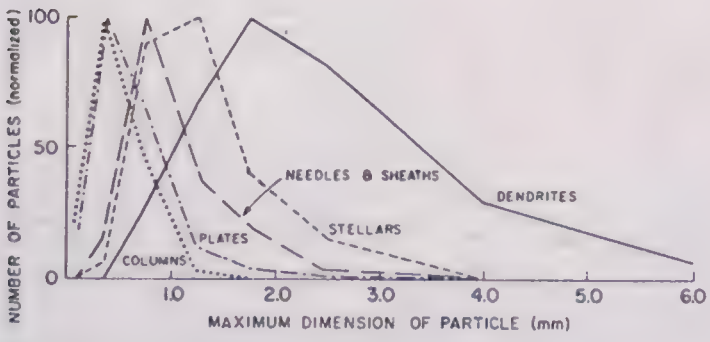

Size distribution of snow crystals collected at Alpental Base, Hyak, and Keechelus Dam, State of Washington. (From Hobbs *et al.*, 1972)

As can be seen the dimensional relationships proposed by various authors agree reasonably well, although they were derived from observations in clouds in different parts of the world.

The microstructure of cirrus type clouds has been studied by Weickman (1945, 1949), Heymsfield (1972, 1975), Heymsfield and Knollenberg (1972).

These studies have revealed a concentration of ice crystals which normally range between 10 and 50 l^{-1}. Bullets, rosettes and columns of mean length between 100 and 1000 μm predominate. Higher concentrations have been found in cirrus resulting from cumulonimbus anvils.

6.2 The growth of ice crystals

Once ice embryos are formed, either by sublimation directly from the vapour or by freezing of a supercooled droplet, growth continues by diffusion in a supersaturated environment. The growth equations are analagous to those of section 3.4 for water droplets, but with an important difference due to the fact that ice crystals are generally not spherical. This difference is treated by noting the similarity between the governing equations and boundary conditions for electrostatic and diffusion problems. As a result the capacitance of the growing crystal enters the growth equation in place of the radius (C=r for a sphere). If an ice crystal is formed in supercooled cloud it grows in an environment close to water saturation. This creates a significant supersaturation with respect to ice. The pressure and temperature dependence of this saturated vapour pressure and the diffusion and thermal conductivity coeeficients is assessed in the form of the normalised growth rate below :

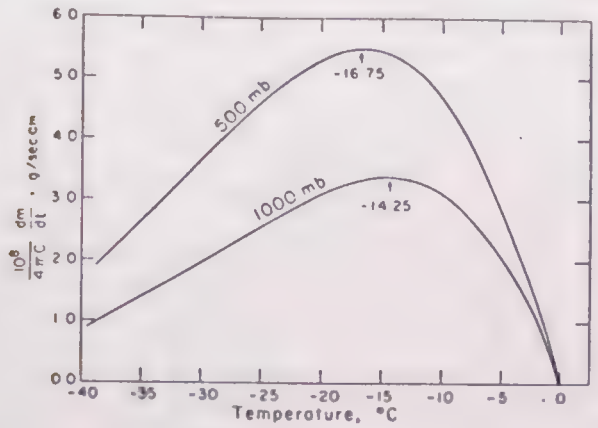

Maximum growth is predicted at a temperature of about -15°C over a wide range of pressures. This is modulated by the effects of the various crystal habits. Miller and Young (1979), Ryan et al (1976) and others have assessed this theoretically and experimentally. It is found that a correction must be applied for the effect of relative movement between the vapour field and crystal (ventilation) and that those crystal forms with a large and convoluted surface area exhibit maximum growth rates.

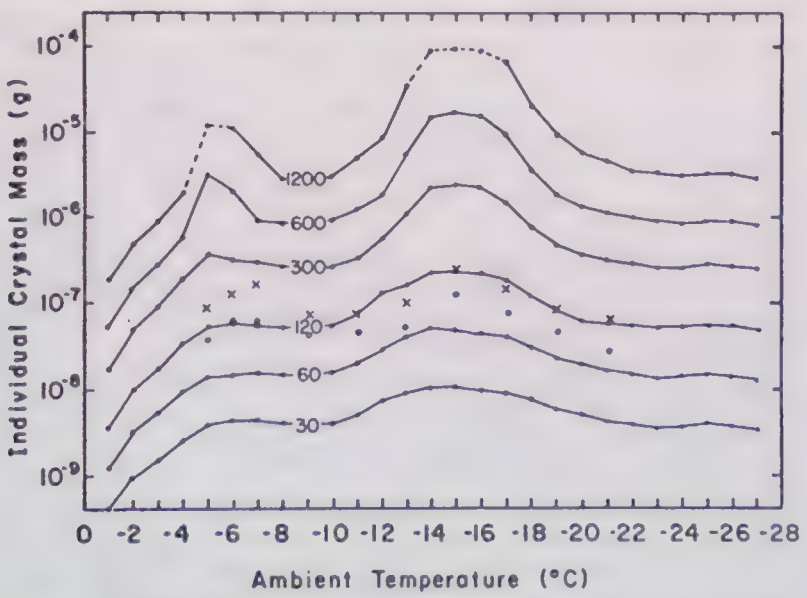

FIG. 8. Predicted average crystal mass after 30, 60, 120, 300, 600 and 1200 s of growth at water saturation and constant temperature. Dashed lines indicate regions where growth had somewhat slowed due to the crystals' major axis reaching the limit of the two-dimensional array. Points indicated by circles and crosses are observations by Ryan *et al.* (1976) at 100 and 150 s, respectively.

The secondary maximum in crystal mass at -5°C is a result of the of the extreme axial ratios and lower densities associated with needle growth. The primary maximum at -15°C arises both from dendritic growth and the maximum in the normalised growth rate.

The same set of equations describe ice crystal evaporation in a subsaturated environment. Roach (1976), Hall and Pruppacher (1977) have considered the survival of ice particles falling from cirrus but found it necessary to include the effects of net radiative cooling of the falling crystals and their ventilation. They have shown that crystals can survive fall distances of up to 2 km when the relative humidity (with respect to water) is less than 70%; larger distances are possible if RH > 70%.

Ice crystals falling through supercooled cloud can grow by accretion. This process leads to rimed structures; aggregation of the ice crystals produces snowflakes. The characteristics of these hydrometers will be described in section 7.3. Here it should be noted that as for drop coalescence, a size and shape dependent collection efficiency influences the process. The threshold for riming is about 300 μm diameter for plates and apparently columns must achieve a thickness of some 50 μm before drops are caught. Reference to the diagram above suggests that vapour growth at water saturation for a few minutes is necessary to achieve such sizes.

7 Precipitation characteristics

Precipitation may be initiated through either the warm coalescence or ice crystal process. After such particles are formed they grow primarily by sweeping out cloud droplets, or by combining with one another. This idea allows definition of the boundary between cloud and precipitation particles as the threshold of coalescence. A necessary if insufficient condition for the latter is an appreciable terminal velocity. Depending upon various factors this continued growth produces raindrops, snowflakes or hail.

7.1 Rain

Regardless of how it is initiated, precipitation over much of the world reaches the ground as rain.

Its most commonly measured characteristic is the rainfall rate at the surface. A more complete description is provided by the drop size distribution function which expresses the number of drops per unit size interval (usually diameter) per unit volume of space. Such distributions have been measured by a variety of methods in most of the world's climatic regions. Though they are variable in time and space the distributions usually indicate a rapid decrease in drop concentration with increase in size, at least for diameters exceeding 1 mm. They generally show a systematic variation with rainfall intensity; the the number of large drops tending to increase with rainfall rate.

Marshall and Palmer (1948) first suggested the use of a negative exponential form for the drop size distribution based on surface observations in Canada. Thus

$$N(D) = N_0 e^{-\Lambda D}$$

where $N(D)dD$ is the number of drops per unit volume with diameters between D and D+dD. They found that the slope factor Λ depends only on rainfall rate and is given by:

$$\Lambda(R) = 41 R^{-0.21}$$

where Λ has units of cm^{-1} and R is measured in mm/hr. Remarkably they also found that the intercept parameter N_0 is a constant given by:

$$N_0 = 0.08 \text{ cm}^{-4}$$

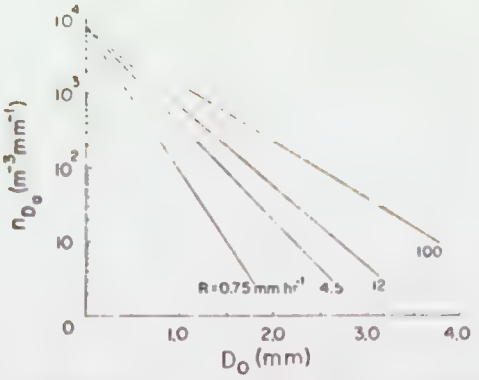

Marshall-Palmer raindrop size distribution. (Based on Marshall and Palmer, 1948)

The particular advantage of the negative expontential derives from the mathematical identity

$$\int_0^\infty D^n N_0 \exp(-\Lambda D)\, dD = \frac{\Gamma(n+1)}{\Lambda^{n+1}}$$

where Γ is the gamma function, n is a real number > -1, $\Lambda > 0$. Then (a) the total number of particles $> d$ per unit volume is

$$N_T(d) = \int_d^\infty N(D)\, dD = \frac{N_0}{\Lambda} e^{-\Lambda D} = 1951\, R^{0.21} e^{-\Lambda d}\ m^{-3}$$

(b) the mass of precipitation water per unit volume of air

$$\omega_p = \rho_L \frac{\pi}{6} \int_0^\infty D^3 N(D)\, dD = \frac{\pi \rho_L N_0}{\Lambda^4} = 9_{10}{}^{-2} R^{0.84}\ g\ m^{-3}$$

(c) the median volume diameter $= \frac{3.67}{\Lambda} = 9\,10^{-2} R^{0.21}$ cm

The Met.Office have adopted the following definitions

Precipitation	R (mm hr^{-1})
Slight Rain	< 0.5
Moderate "	0.5 – 4
Heavy "	> 4
Slight Shower	< 2
Moderate "	2 – 10
Heavy "	10 – 50
Violent "	> 50

It is instructive to assess the numerical values of some of the moments of the dropsize distribution against these definitions.

R (mm hr^{-1})	Λ (cm^{-1})	$d_{½}$ (mm)	$N_{d_{½}}$ (m^{-3})	$N_{d=1mm}$ (m^{-3})	ω_p (g m^{-3})
0.5	47	0.8	27	15	0.05
2	35	1.0	58	65	0.16
4	31	1.2	67	122	0.28
10	25	1.4	81	252	0.62
20	22	1.7	94	409	1.1
50	18	2.0	114	735	2.4
100	16	2.4	130	1077	4.3

The median volume diameter varies over a rather small range through the whole span of likely rainfall rates. Note also that rather small amounts of liquid water are tied up in precipitation size particles. (Recall that quite innocuous clouds have liquid water contents $\sim 0.5\ gm^{-3}$). The number of drops greater than 1 mm is typically a few hundred per m^{-3}.

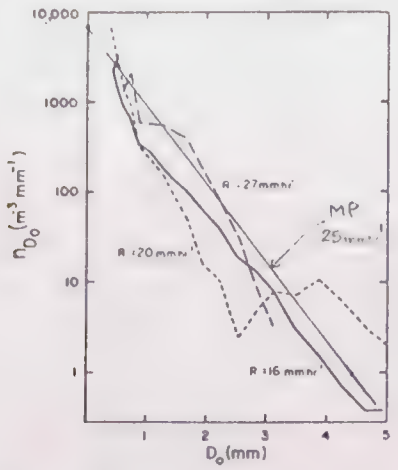

Raindrop size distribution observed on three different occasions in southern Switzerland. (From Joos *et al.*, 1968)

For steady rain at the surface in continental mid-latitudes the M-P values of Λ and N_0 are often found to be reasonable approximations for drops, $D \geq 1$ mm. However it has been pointed out by Joss and Gori (1978) that departures from the exponential form, towards a more monodisperse distribution, are found in surface data when averaging periods become small. (~ 1 min or 0.5 km scale). Plank et al (1980) have found that the exponential form is satisfactory for averaging periods ≥ 10 sec (1 km scale) in aircraft traverses through widespread rain but in showery conditions a much greater tendency to monodispersity is evident, even over averaging periods as long as 100 sec (10 km scale). Radar reflectivity is proportional to $\int_0^\infty D^6 N(D)\, dD$; being very sensitive to the concentration of a few large drops therefore. Data from radar studies of rain suggest that significant departures from the MP values of N_0 and Λ are to be expected in individual rain events.

A raindrop falling in still air reaches its steady terminal velocity when the aerodynamic drag force is balanced by the weight of the drop; the Archemedian upthrust of the air being negligible. For a spherical drop of diameter D and density ρ_L

$$\frac{\pi}{4} D^2 \cdot \frac{1}{2} C_D \rho_a V^2 = \frac{\pi}{6} D^3 \rho_L g$$

or $$V = \sqrt{\frac{4}{3} \rho_L g D / \rho_a C_D}$$

where C_D is a function of the Reynolds number $(VD\rho_a/\eta_a)$ of the flow ρ_a, η_a are the density and viscosity of the air.

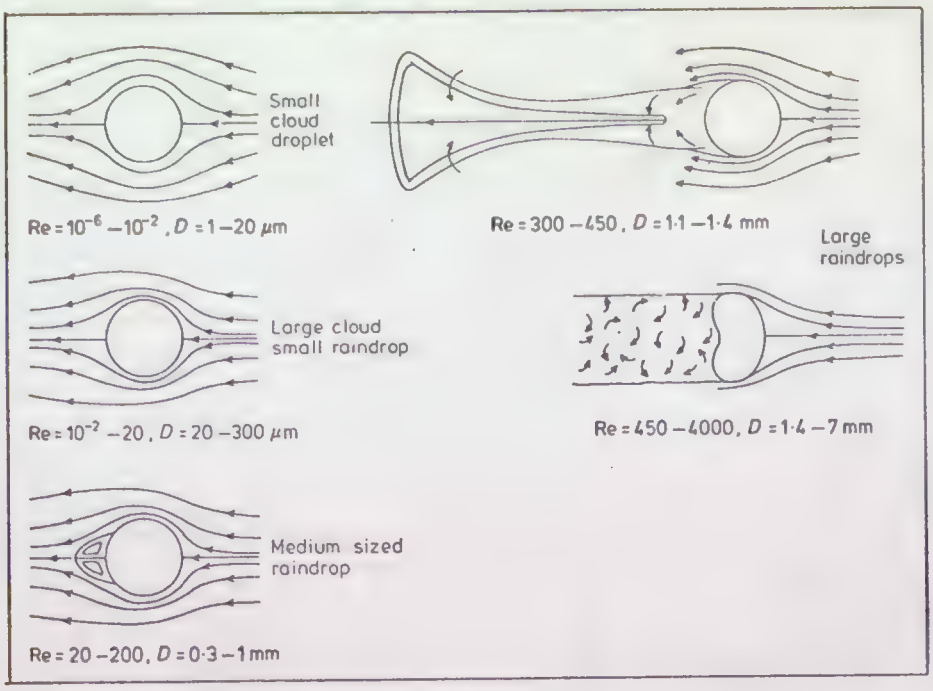

The figure above shows how Re and the air flow pattern vary through the range of drop sizes relevant to cloud physics. For medium sized raindrops a closed vortex begins to form behind the drop. Larger drops detach these vortices periodically from the opposite sides of the wake axis, producing an unsteady motion. For drops D > 1.5mm, the wake becomes increasingly turbulent and they become progressively flattened. The drag coefficient then becomes considerably greater than th at of the equivalent rigid sphere. Terminal velocities increase correspondingly slowly with diameter, as shown below. The data are appropriate to sea level.

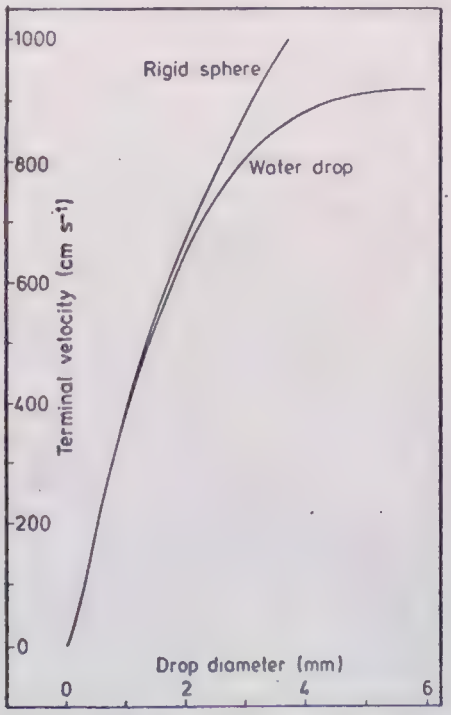

Drops disrupt when the force of aerodynamic drag exceeds that due to hydrostatic and surface tension restoring forces. In the atmosphere where unbalanced turbulent motions are to be expected this occurs at about D = 6 mm.

An explanation of the tendancy for drop size distributions to approach a negative exponential form is provided, in part at least

by this phenomenon of break up. A number of small drops are produced at disruption thereby recycling water in a direction opposite to that of coalescence. Another cause of breakup is collision between drops when the rotational kinetic energy of the product exceeds the surface energy required to generate separated drops. Brazier-Smith et al (1972) have worked out the details of this. Again disruption produces small satellite drops. Young (1975) has attempted to model evolution of the drop size distribution taking these effects into account, with reasonable success.

7.2 Snow

As snowflakes are irregular aggregates of crystals or smaller snowflakes there is no easy way to measure and characterise their linear dimensions. Consequently snowflake sizes are usually expressed in terms of particle mass, or equivalently the diameter of the water drop formed when the snowflakes melt. The data of Gunn and Marshall(1958) show that the size of snowflakes defined in this way can be fitted reasonably well by an exponential function of the form shown below.

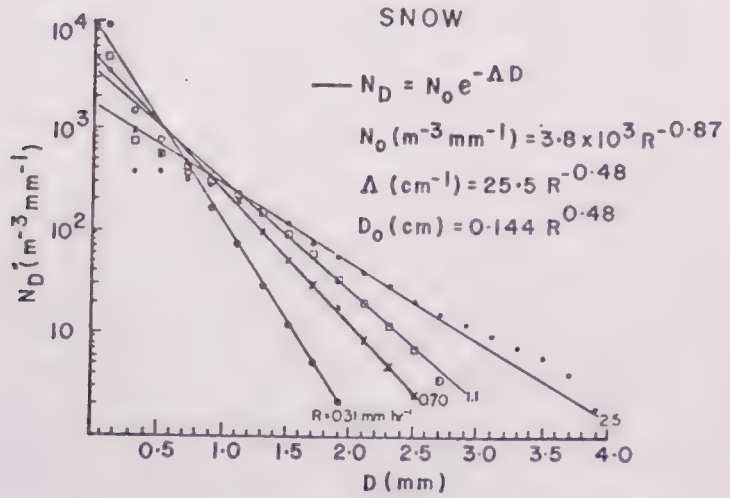

The precipitation rate (mm hr^{-1}) is in terms of water equivalent depth of accumulated snow.

In a study of frontal precipitation Houze et al (1979) have attempted to characterise the dimensions of shadowgraphs of individual hydrometers observed at various temperatures in cloud. Again the data were well fitted by a negative exponential; for larger particles at least. The observed variation of Λ and No are as shown below.

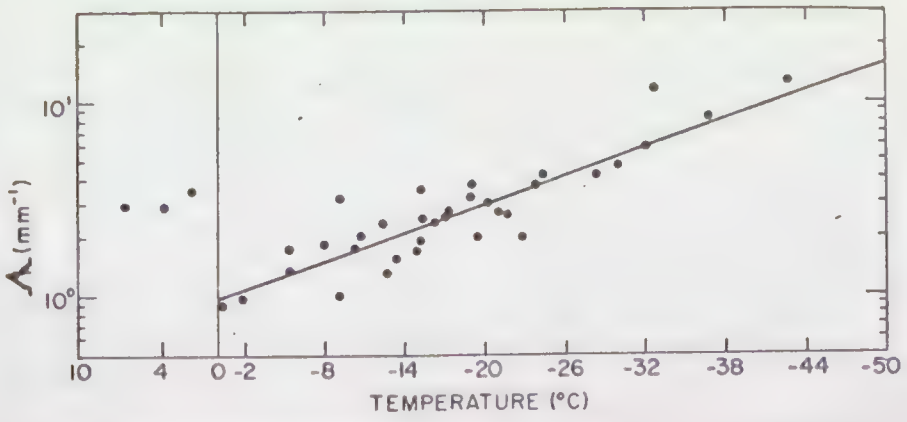

Variation with temperature of the slope parameter Λ of the Marshall-Palmer distributions fitting the large-particle ($D \geq D_0$) part of all of the observed particle-size spectra. The best-fit line computed for temperatures <0°C has a correlation coefficient of −0.90.

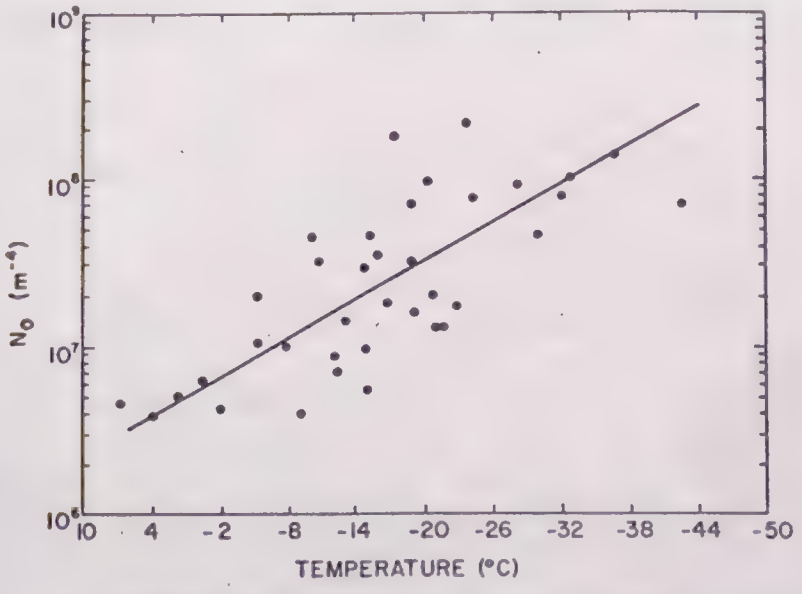

Variation with temperature of the intercept parameter N_0 of the Marshall-Palmer distributions fitting the large-particle ($D \geq D_0$) part of all of the observed particle-size spectra. The best fit line computed by the method of least squares has a correlation coefficient of −0.66.

The change in Λ is consistent with the growth of ice particles by accretion and aggregation. Passage through the melting zone is reflected by a sudden reduction in the mean particle size and hence increase in Λ (Recall that $d_{\frac{1}{2}} = 3.67/\Lambda$). N_0 is observed to increase with temperature; again in keeping with accretional growth.

The terminal velocities of ice crystals, and snowflakes have been measured as a function of their linear dimensions by Nakaya and Terada. Their results are presented in the attached figures.

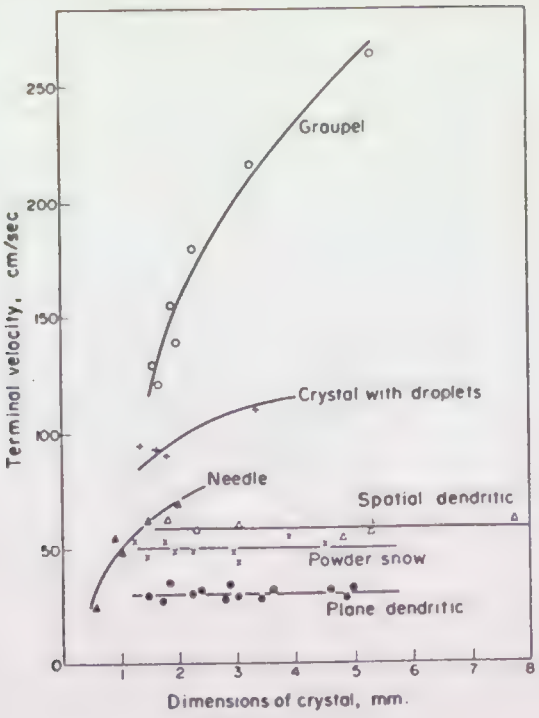

Density of snowflakes as a function of their mean diameter

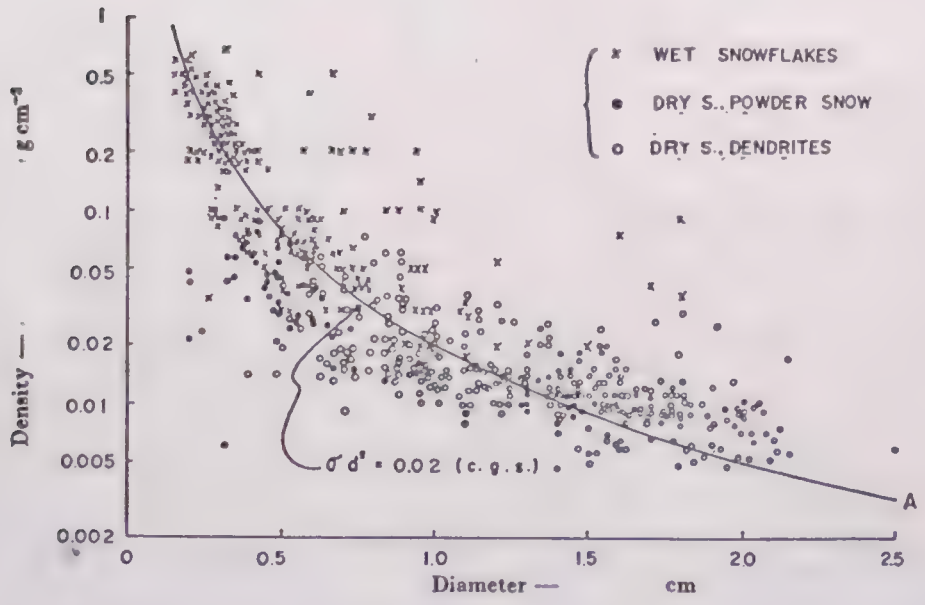

Figure (*b*.2) — Terminal velocity of fall of snowflakes as a function of their density

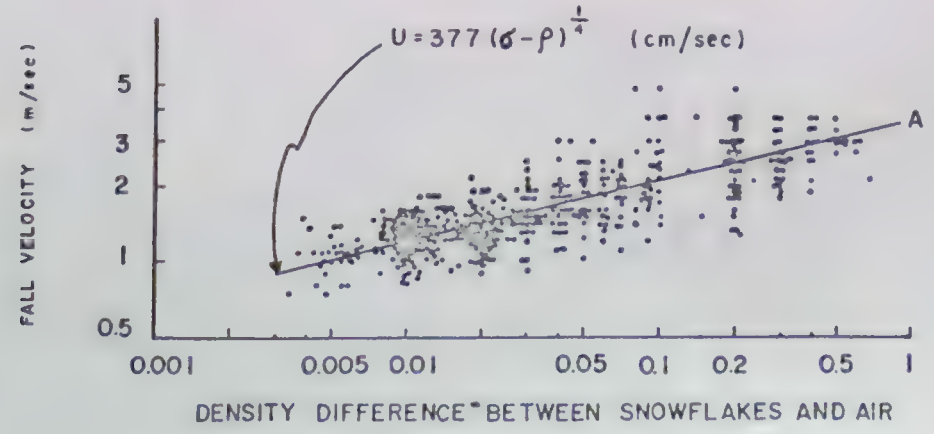

7.3 Graupel and Hail

When riming of an ice particle has proceeded to a stage where the features of the primary ice particle are only faintly or no longer visibly the hydrometeor is called a graupel particle. It has a white, opaque and fluffy appearance due to the presence of a large number of air capillaries in the ice structure. In the later stages of riming such particles may have a conical, rounded or irregular shape. Ice particles are called hailstones if their maximum dimensions are typically larger than 5 mm. They have a roundish, ellipsoidal or conical shape often with lobes or other proturbances. In cross-section they exhibit an onion type layered structure with alternating opaque and clear layers caused by the presence of more or less numerous air bubbles.

An important aspect of hail growth is the latent heat of fusion released when the accreted water freezes. Owing to this heating, the temperature of a growing haistone is several degrees warmer than its cloud environment. When the surface of the hailstone is at subfreezing temperature, the collected water droplets freeze quickly and the surface remains essentially dry. When the surface is at 0°C the collected water does not freeze immediately and the surface is wet. Some may be shed, but the remainder forms 'spongy ice'. During its lifetime a stone may undergo alternate wet and dry growth as it passes through a cloud of varying temperature and liquid water content, thus developing the layered structure that is often observed. Much research effort has been spent in trying to disentangle a hailstone's quantitative history from this structure.

Auer (1972) has summarised measurements reported in the literature on the size distribution of hailstones and graupel particles.

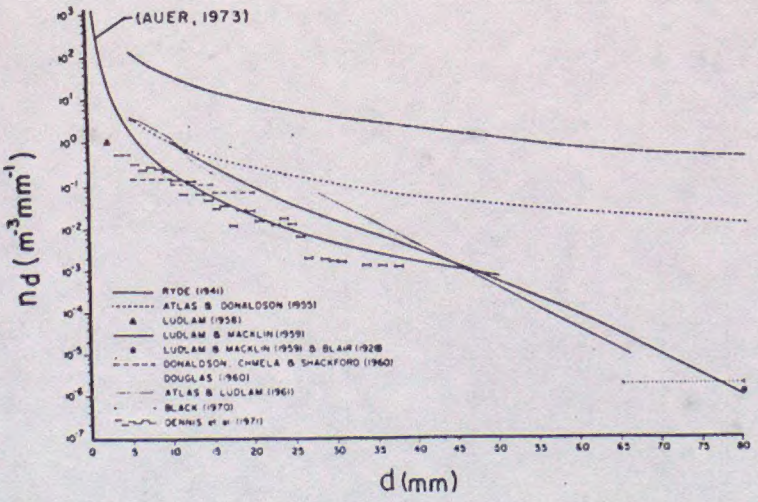

Number concentration of graupel particles and hailstones as a function of their diameter.

Federer and Waldvogel (1975) found the size distribution of spherical haistones which fell from storms over central Switzerland followed the negative exponential relationship with

$$1.5 \leq N_0 \leq 52 \text{ m}^{-3} \text{ mm}^{-1} \quad \text{and} \quad 0.33 \leq \Lambda \, 0.64 \text{ mm}^{-1} \quad \text{for } D \leq 22 \text{ mm}$$

The hail fall rates ranged between 2.6 and 152 mm hr^{-1}. Ross (1972) reported a single haistone which weighed 766 g and had a circumference of 44 cm.

The completed terminal velocity of smooth solid spheres as a function of their diameter and density is shown below.

— Terminal velocity of fall of smooth spheres as a function of their diameter (computed)

v : terminal velocity
d : diameter

S.G. : specific gravity ≈ density in g cm^{-3}

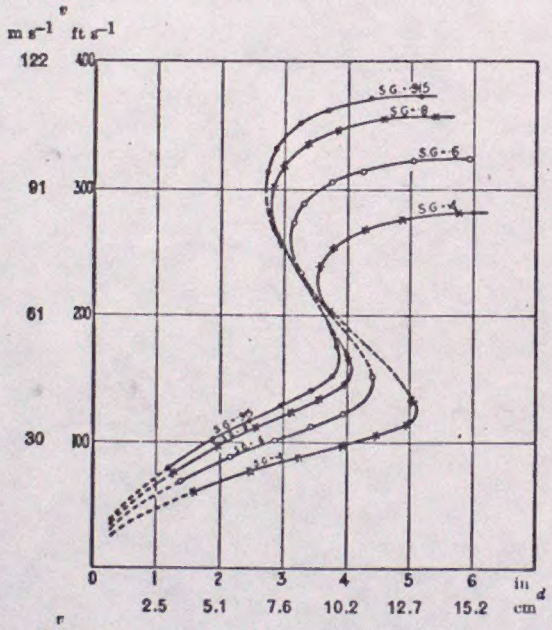

Ground level

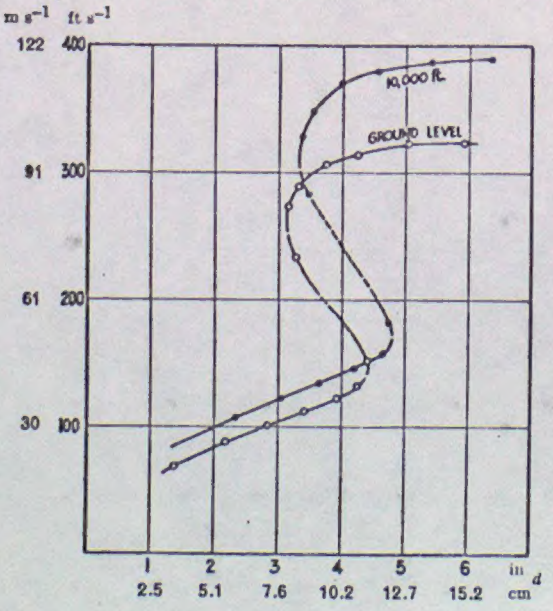

Ground level and 10 000 ft (3 048 m) level — specific gravity ≈ density = 0.6 g cm^{-3}

References

Auer, A H, 1972: Month. Wea. Rev., 100, 325

Berry, E X, 1968: J. Atmos. Sci., 25, 151

Berry, E X, & Reinhardt, R L, 1974: J Atmos. Sci., 31, 1825

Brazier-Smith, P R, Jennings, S G & Latham, J, 1972: Proc. Roy. Soc, A326, 393

Federer, B & Waldvogel, A 1975: J. Appl. Meteor., 14, 91

Gagin, A 1971: Proc. Weather Mod. Conf. Canberra, 5

Gunn, R & Marshall, J S, 1958: J. Meteor., 15, 452

Hall, W D & Pruppacher, H R, 1977: J. Atmos. Sci,33, 1995

Heymsfield, A, 1972: J. Atmos. Sci, 29, 1348

Heymsfield, A, 1975: J.Atmos. Sci, 32, 809

Heymsfield, A & Knollenberg, R E, 1972: J.Atmos. Sci, 21, 1358

Hobbs, P V et al 1974: Res. Rpt No VII, Dept Atmos. Sci, University of Wash.

Joss, J & Gori, E G, 1978: J.Appl. Meteor. 17, 1054

Joss,J , Thomas, J C & Waldvogel,A 1968: Proc. Cloud Physics Conf, Toronto, 369

Levin,Z, et al, 1980: Proc Cloud Physics Conf, Clermont Ferrand, 45

Marshall, J S & Palmer W M , 1948: J Meteor, 5, 165

Mason, B J, 1978: Phys Bull, 29, 364

*Mason, B J, 1971: The Physics of Clouds, Oxford

Miller, T L & Young,K C, 1979: J Atmos Sci, 36, 458

Magono, C & Lee, C W, 1966 J Fac Sci, Hokkaido Univ. Ser 7, 2, No 4

Plank, V G,
Berthel, R O &
Delgado, L V, 1980: VIII Cloud Physics Conf, 173

*Pruppacher, H R &
Klett, J D 1978: Microphysics of Cloud & Precipitation, D Reidel

Roach, W T &
Bader, M, 1976: Proc. Radiation Atmos, Garmisch, 239

*Rogers, R R, 1977: A Short Course in Cloud Physics, Pergamon

Ryan, E F,
Wishart, E F &
Shaw, D E 1976: J Atmos Sci, 33, 842

Schnell, R C &
Vali, G 1976: J Atmos Sci, 28, 402

*Twomey, S 1977: Atmospheric Aerosols, Elsevier

Vali, G et al 1976: J Atmos Sci, 28, 410

Weickman, H K, 1945: Beitr.Z.Phys.d.freien Atmosphare, 28, 12

Weickman, H K, 1949: Ber. Deutsch. Wett. Dienst.U S Zone, Nr 6

Young, K C, 1975: J Atmos Sci, 32, 965

* Particularly useful general reference works.